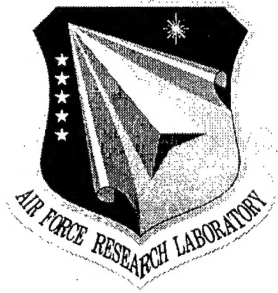


**AFRL-IF-RS-TR-2001-100**  
**Final Technical Report**  
**May 2001**



## **A GENERIC MICROFLUIDIC SYSTEM FOR REMOTE SENSORS**

**University of Cincinnati**

**Sponsored by**  
**Defense Advanced Research Projects Agency**  
**DARPA Order No. E935**

*APPROVED FOR PUBLIC RELEASE; DISTRIBUTION UNLIMITED.*

The views and conclusions contained in this document are those of the authors and should not be interpreted as necessarily representing the official policies, either expressed or implied, of the Defense Advanced Research Projects Agency or the U.S. Government.

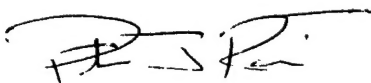
**AIR FORCE RESEARCH LABORATORY**  
**INFORMATION DIRECTORATE**  
**ROME RESEARCH SITE**  
**ROME, NEW YORK**

**20010810 028**

This report has been reviewed by the Air Force Research Laboratory, Information Directorate, Public Affairs Office (IFOIPA) and is releasable to the National Technical Information Service (NTIS). At NTIS it will be releasable to the general public, including foreign nations.

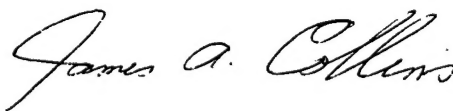
AFRL-IF-RS-TR-2001-100 has been reviewed and is approved for publication.

APPROVED:



PETER J. ROCCI  
Project Engineer

FOR THE DIRECTOR:



JAMES A. COLLINS, Acting Chief  
Information Technology Division  
Information Directorate

If your address has changed or if you wish to be removed from the Air Force Research Laboratory Rome Research Site mailing list, or if the addressee is no longer employed by your organization, please notify AFRL/IFTD, 525 Brooks Road, Rome, NY 13441-4505. This will assist us in maintaining a current mailing list.

Do not return copies of this report unless contractual obligations or notices on a specific document require that it be returned.

A GENERIC MICROFLUIDIC SYSTEM  
FOR REMOTE SENSORS

Chong H. Ahn, H. Thurman Henderson,  
William R. Heineman, H. Brian Halsall,  
Joseph H. Nevin, and Arthur J. Helmicki

Contractor: University of Cincinnati  
Contract Number: F30602-97-2-0102  
Effective Date of Contract: 01 May 1997  
Contract Expiration Date: 30 September 2000  
Short Title of Work: A Generic Microfluidic System  
For Remote Sensors  
Period of Work Covered: May 97 - Sep 00  
  
Principal Investigator: Chong H. Ahn  
Phone: (942) 824-6429  
AFRL Project Engineer: Peter J. Rocci  
Phone: (315) 330-4654

APPROVED FOR PUBLIC RELEASE; DISTRIBUTION  
UNLIMITED.

This research was supported by the Defense Advanced Research  
Projects Agency of the Department of Defense and was monitored  
by Peter j. Rocci, AFRL/IFTD, 525 Brooks Road, Rome, NY.

| REPORT DOCUMENTATION PAGE   |   |  | Form Approved<br>OMB No. 0704-0188   |   |
|---|---|--|--|---|
| <small>Public reporting burden for this collection of information is estimated to average 1 hour per response, including the time for reviewing instructions, searching existing data sources, gathering and maintaining the data needed, and completing and reviewing the collection of information. Send comments regarding this burden estimate or any other aspect of this collection of information, including suggestions for reducing this burden, to Washington Headquarters Services, Directorate for Information Operations and Reports, 1215 Jefferson Davis Highway, Suite 1204, Arlington, VA 22202-4302, and to the Office of Management and Budget, Paperwork Reduction Project (0704-0188), Washington, DC 20503.</small>   |   |  |  |   |
| 1. AGENCY USE ONLY (Leave blank)  |   | 2. REPORT DATE<br>MAY 2001                                 |  | 3. REPORT TYPE AND DATES COVERED<br>Final May 97 - Sep 00 |
| 4. TITLE AND SUBTITLE<br>A GENERIC MICROFLUIDIC SYSTEM FOR REMOTE SENSORS   |   |  | 5. FUNDING NUMBERS<br>C - F30602-97-2-0102<br>PE - 63739E<br>PR - E117<br>TA - 00<br>WU - 20 |   |
| 6. AUTHOR(S)<br>Chong H. Ahn, H. Thurman Henderson, William R. Heineman, H. Brian Halsall, Joseph H. Nevin, and Arthur J. Helmicki  |   |  |  |   |
| 7. PERFORMING ORGANIZATION NAME(S) AND ADDRESS(ES)<br>University of Cincinnati<br>PO Box 210030<br>Cincinnati Ohio 45221  |   |  | 8. PERFORMING ORGANIZATION<br>REPORT NUMBER<br><br>N/A                                       |   |
| 9. SPONSORING/MONITORING AGENCY NAME(S) AND ADDRESS(ES)<br>Defense Advanced Research Project Agency    Air Force Research Laboratory/IFTD<br>3701 North Fairfax Drive                                525 Brooks Road<br>Arlington Virginia 22203-1714                        Rome New York 13441-4505   |   |  | 10. SPONSORING/MONITORING<br>AGENCY REPORT NUMBER<br><br>AFRL-IF-RS-TR-2001-100              |   |
| 11. SUPPLEMENTARY NOTES<br>Air Force Research Laboratory Project Engineer: Peter J. Rocci/IFTD/(315) 330-4654   |   |  |  |   |
| 12a. DISTRIBUTION AVAILABILITY STATEMENT<br>APPROVED FOR PUBLIC RELEASE; DISTRIBUTION UNLIMITED.  |   |  | 12b. DISTRIBUTION CODE   |   |
| 13. ABSTRACT (Maximum 200 words)<br>The objective of this project is to develop a generic MEMS-based microfluidic system for portable biochemical detection systems. To achieve this goal, an innovative generic MEMS-based microfluidic system has been designed, fabricated, and characterized, and successfully applied to a portable all in one biochemical detection system. The analytical concept is based on an immunoassay with electrochemical detection. Microbead technology is adopted for both sampling and detection to trap and manipulate the target. Through the project, a portable integrated biochemical detection system, which has sampling and detection capabilities, has been successfully developed and characterized for the sampling and detection of 50 ng/ml of antigen concentration in 20 minutes of total assay time. |   |  |  |   |
| 14. SUBJECT TERMS<br>Microfluidic Systems   |   |  | 15. NUMBER OF PAGES<br>118   |   |
|   |   |  | 16. PRICE CODE   |   |
| 17. SECURITY CLASSIFICATION<br>OF REPORT<br>UNCLASSIFIED  | 18. SECURITY CLASSIFICATION<br>OF THIS PAGE<br>UNCLASSIFIED | 19. SECURITY CLASSIFICATION<br>OF ABSTRACT<br>UNCLASSIFIED | 20. LIMITATION OF<br>ABSTRACT<br>UL  |   |



## Table of Contents

|  |    |
|--|----|
| I. Executive Summary.....  | 1  |
| II. Problem Definition.....  | 5  |
| Microfluidic Components and Systems .....                                | 5  |
| Biochemical Assays .....   | 5  |
| Electronic Control and Analysis System .....                             | 6  |
| III. Approaches .....  | 7  |
| MEMS Components and Microfluidic Systems .....                           | 7  |
| Meso/Automated Components and Systems Approach.....                      | 7  |
| Microfabricated Components and Systems Approach.....                     | 13 |
| Biochemistry and Electrochemical Detection.....                          | 29 |
| Electronic Circuitry and Control Systems .....                           | 33 |
| IV. Problems Encountered .....   | 39 |
| Microfluidic Components and Systems .....                                | 39 |
| Biochemical Assays .....   | 40 |
| Microcontroller Based Electronic System .....                            | 43 |
| V. Lessons Learned.....  | 44 |
| Microfluidic Components and Systems .....                                | 44 |
| Biochemical Assays .....   | 44 |
| Microcontroller Based Electronic System .....                            | 45 |
| VI. Results.....   | 46 |
| Automated Integrated Microfluidic Systems for Biochemical Detection..... | 46 |
| Integrated Microfluidic System for Biochemical Detection .....           | 49 |
| VII. Conclusions .....   | 55 |
| VIII. APPENDICES .....   | 57 |

## Table of Figures

|  |    |
|--|----|
| Figure I-1: A proposed generic microfluidic system for biochemical detection .....   | 1  |
| Figure I-2: Analytical concept based on sandwich immunoassay and electrochemical<br>detection.....   | 1  |
| Figure I-3: Conceptual illustration of bio-sampling and immunoassay procedure.....   | 2  |
| Figure I-4: Developed microfluidic systems for magnetic bead-based biochemical<br>detection.....   | 4  |
| Figure III-1: (a) Realized meso-system, and (b) corresponding control software panel ...   | 7  |
| Figure III-2: Valve with magnetic spring .....   | 8  |
| Figure III-3: Valve with “cricket like” spring.....  | 8  |
| Figure III-4: Magnetic Separator .....   | 9  |
| Figure III-5: Photograph of the micro wire electrode .....   | 9  |
| Figure III-6: Microphotograph of the micromachined IDA.....  | 10 |
| Figure III-7: Polyethylene/Teflon reservoirs with stirrer.....   | 11 |
| Figure III-8: Photograph of the valveless mini rotary pump .....   | 11 |
| Figure III-9: Schematic of the micro flow channel with indication of velocity profile,<br>thermal boundary layer and virtual sensors ..... | 12 |
| Figure III-10: Relative change of the sensor output voltage as a function of flow rate for<br>different input currents.....                | 12 |
| Figure III-11: Output voltage is plotted as a function of time for different input current<br>levels and with varying flow rates .....     | 13 |
| Figure III-12: Conceptual illustration of bio-sampling and immunoassay procedure.....  | 14 |
| Figure III-13: Schematic illustration of the designed biofilter with embedded serpentine<br>inductor structure .....                       | 14 |
| Figure III-14 (a): Schematic illustration of the surface-mountable biofilter .....   | 15 |
| Figure III-14 (b): Schematic illustration of the surface-mountable biofilter .....   | 15 |
| Figure III-15: Enzymatic kinetics for electrochemical detection of the immunosensor...   | 16 |
| Figure III-16: Design layout of the electrochemical immunosensor .....   | 17 |
| Figure III-17: Microphotograph of the integrated biofilter and biosensor .....   | 18 |
| Figure III-18: Separation test results.....  | 18 |
| Figure III-19: Measured maximum fluid velocity and flow rate .....   | 19 |
| Figure III-20: Calibration curve of the electrochemical immunosensor for different PAP<br>concentration.....                               | 20 |
| Figure III-21: SEM photographs of micromachined solenoid-type inductors.....   | 20 |
| Figure III-22: Photographs of fabricated solenoid-type inductor .....  | 21 |
| Figure III-23: Several versions of microvalves using magnetic microinductors .....   | 22 |
| Figure III-24: Pinch-type microvalve .....   | 22 |
| Figure III-25: Measured flow rate of mesa membrane-type microvalves with valve seats<br>.....  | 23 |
| Figure III-26: Experimental results of pinch-type microvalve .....   | 23 |
| Figure III-27: Surface mountable pinch-type micropump .....  | 24 |
| Figure III-28: Pump rate as a function of back pressure with various driving frequencies<br>.....  | 24 |
| Figure III-29: Schematic illustration of the surface mounting technique on a fluidic<br>motherboard .....                                  | 25 |

|   |    |
|---|----|
| Figure III-30: Schematic diagram of serial interconnects.....   | 26 |
| Figure III-31: Microphotographs of serial interconnects.....  | 26 |
| Figure III-32: Flow rate versus pressure drop.....  | 27 |
| Figure III-33: Developed reservoir using elastic silicone compound and sealed with PDMS.....                      | 28 |
| Figure III-34: Reservoir mounted on the plastic based microfluidic system.....                                    | 28 |
| Figure III-35: Magnetic beads .....   | 29 |
| Figure III-36: RDE detection results.....   | 32 |
| Figure III-37: Different immunomagnetic bead spots and corresponding SECM.....                                    | 32 |
| Figure III-38: Block diagram of the microcontroller based electronic system.....                                  | 34 |
| Figure III-39: Stacked microcontroller based electronic system .....  | 35 |
| Figure III-40: Graphical user interface for biochemical detection .....   | 37 |
| Figure VI-1: Packaged microfluidic systems.....   | 46 |
| Figure VI-2: Current-time plots for detection of PAP concentrations.....  | 47 |
| Figure VI-3: Anodic peak current.....   | 47 |
| Figure VI-4: Assay calibration curve of amperometric sensing current peaks versus concentration of mouse IgG..... | 48 |
| Figure VI-5: Integrated microfluidic systems on 3" glass microfluidic motherboards ....                           | 49 |
| Figure VI-6: Integrated microfluidic system for biochemical detection .....                                       | 49 |
| Figure VI-7: Plastic based microfluidic system for biochemical detection.....                                     | 50 |
| Figure VI-8: Microphotograph of the integrated biofilter and biosensor .....                                      | 51 |
| Figure VI-9: Calibration curve of the electrochemical immunosensor for PAP solution.                              | 51 |
| Figure VI-10: Magnetic beads .....  | 52 |
| Figure VI-11: Immunoassay results measured by amperometric time-based detection method.....                       | 53 |
| Figure VI-12: Four repeated immunoassays for 50 ng/ml of antigen concentrations .....                             | 53 |
| Figure VI-13: Measurement result after release magnetic beads.....  | 54 |

### List of Tables

|   |    |
|---|----|
| Table III-1: Pressure drops for interconnects | 27 |
| Table VI-1: Magnetic beads                    | 52 |

## I. Executive Summary

The general objective of this project is to develop a generic MEMS-based microfluidic system for portable biochemical detection systems. To achieve this goal, an innovative generic MEMS-based microfluidic system has been designed, fabricated, and characterized, and successfully applied to a portable biochemical detection system. This all in one system has achieved sampling and detection capabilities desired for extremely low biochemical concentrations.

Figure I-1 shows a proposed system for the project. The analytical concept is based on an immunoassay with electrochemical detection. Microbead technology is adopted for both sampling and detection to trap and manipulate the target molecules as shown in Figures I-2 and I-3. In this project, magnetic beads have been used for immobilization surfaces as well as carriers of target bio-molecules.

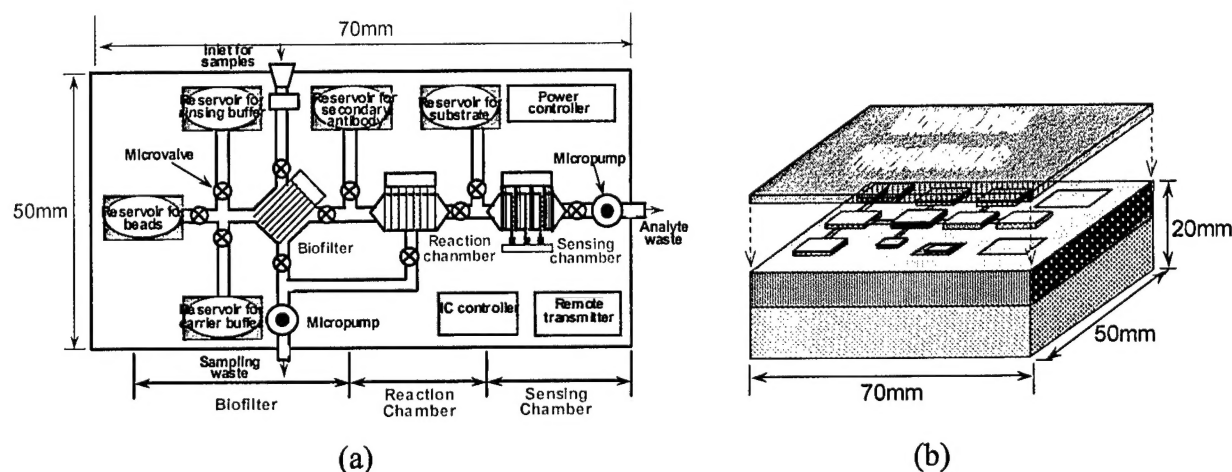


Figure I-1: A proposed generic microfluidic system for biochemical detection

(a) System layout and (b) conceptual illustration of the system.

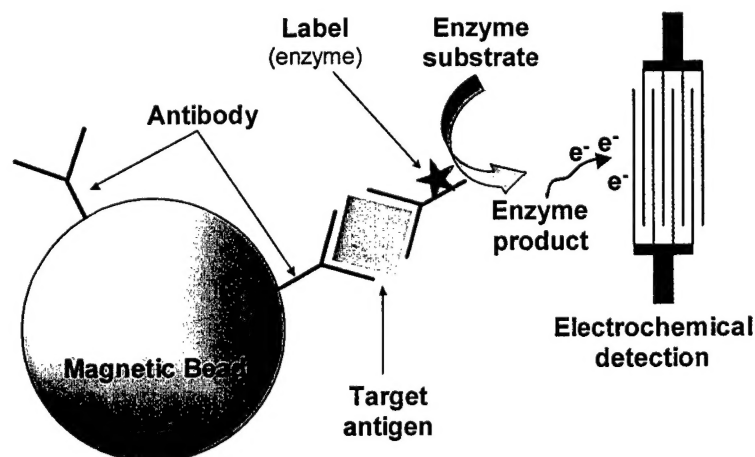
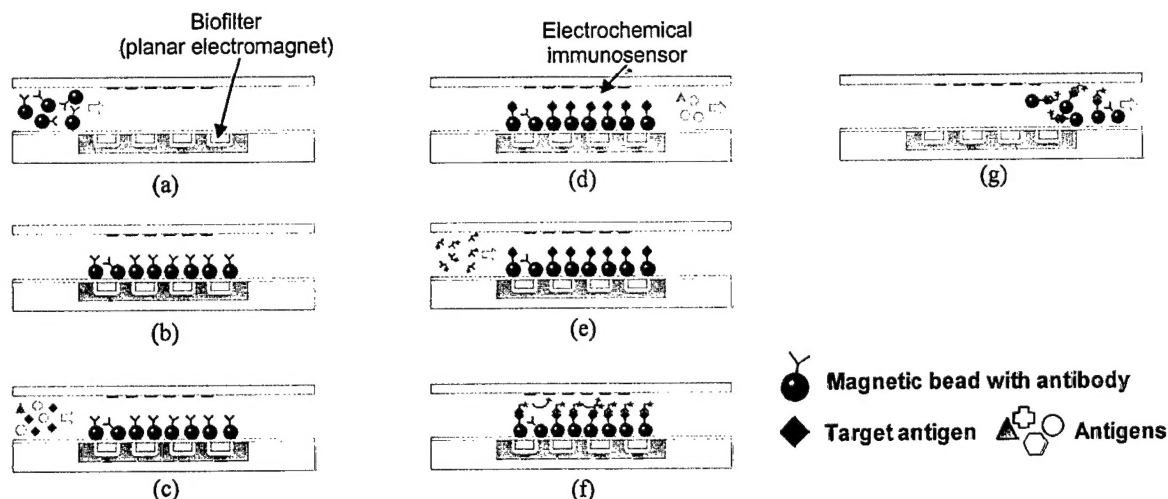


Figure I-2: Analytical concept based on sandwich immunoassay and electrochemical detection



**Figure I-3: Conceptual illustration of bio-sampling and immunoassay procedure**

(a) injection of magnetic beads; (b) separation and holding of beads; (c) flowing samples; (d) immobilization of target antigen; (e) flowing labeled antibody; (f) electrochemical detection; and (g) washing out magnetic beads and ready for another immunoassay.

The development of microfluidic systems is an essential part of the project. The major aspects of the microfluidic systems were to control fluids or samples to be analyzed and to deliver any biochemical samples into reaction/sensing chambers. The desire for using a microfluidic system in biochemical analysis/detection applications is that 1) it requires small volume of samples and reagents and 2) it promises fast analysis/detection. The targeted time for analysis was proposed to be approximately 20 minutes or faster, which would be a revolutionary achievement compared to a required time of 4-5 hours for a conventional biochemical detection system.

To realize the microfluidic systems, several microfluidic components such as microvalves, magnetic biofilters, flow sensors, reservoirs, and microfluidic motherboards have been designed, fabricated and characterized. In addition, microfluidic integration techniques also have been developed, which includes wafer-to-wafer or device-to-wafer bonding techniques and microfluidic interconnection techniques. Several new prototype microfluidic devices have been developed and characterized as an individual component toward a fully integrated microfluidic system on a fluidic motherboard. Consideration on integration and biochemical compatibility issues has been extensively explored to achieve the project goal. A microfluidic motherboard approach has been adopted to integrate individually developed microfluidic components such as biofilters, microvalves/pumps, flow sensors, reservoirs, and reaction/sensing cells. A new material like spin-on Teflon™ has been investigated as a device-to-wafer and/or wafer-to-wafer bonding layer. Since both microvalves and biofilters are magnetically operated, magnetic microinductors based on UV-LIGA technique have been extensively investigated and improved to meet the desired functions.

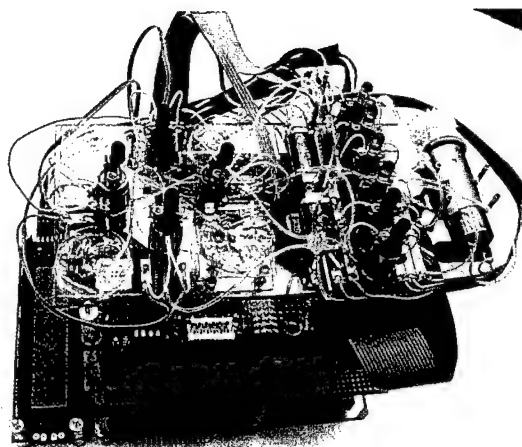
The sensing and detecting format for the biochemical detection set by the biochemistry group was a sandwich immunoassay using electrochemical detection with the antibody capture surface being on magnetic microbeads. In developing magnetic bead-based assay, various types of molecular linkers have been investigated to improve the speed, capacity and interchangeability of magnetic bead function. Applicability of the bead-based assay to the different types of analyte target has been explored for protein toxin, virus, bacterial spore, and bacterium. Small volume rapid methods of electrochemical assay on microbeads have been also developed for the purpose of magnetic bead-based assay development. The electrochemical immunosensor sensitivity has been enhanced with specially designed microelectrodes configuration and electronic control.

The electronic systems were used for the control of microfluidic components (i.e. sequence of microvalves, biofilters), data capture (i.e. electric signal from immunosensor) and analysis aspects of the research. The microfluidic system consisted of up to 10 individual devices that had to be controlled sequentially and rapidly. Additionally, the electrochemical detection principle required highly sensitive analyzing circuitry, called a *potentiostat*, since the signal level from the electrochemical immunosensor is extremely low. To fulfill these requirements toward a generic microfluidic hand-held system for biochemical detection, a microcontroller board was developed with microvalve controllers, potentiostat, AD/DA converter, display unit, and a PC interface board. The system was designed around the main microcontroller board to manage the system operation once programmed. All parts of the electronic and control system were built using printed circuit boards to minimize the system size and to optimize performance. The stack of boards was compact and made a unit suitable for field testing. The complete units were tested and used for biochemical assays in several cases.

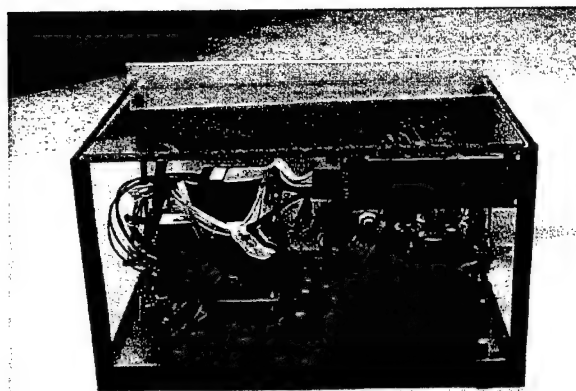
Combining microfluidic systems, electronic/control circuit systems, and biochemical assays, several stand-alone prototype microfluidic systems for magnetic bead-based biochemical detection have been designed, developed and fully characterized to meet the goal of the project. These systems are shown in Figure I-4.

The developed final systems have been successfully characterized by performing full immunoassays as a proof concept of the system using mouse immunoglobulin G (IgG) as a simulant of bio-warfare toxic agent. Immunoreactant consumed during one immunoassay was as low as 10  $\mu$ l and total assay time was less than 20 minutes including all incubation and detection steps.

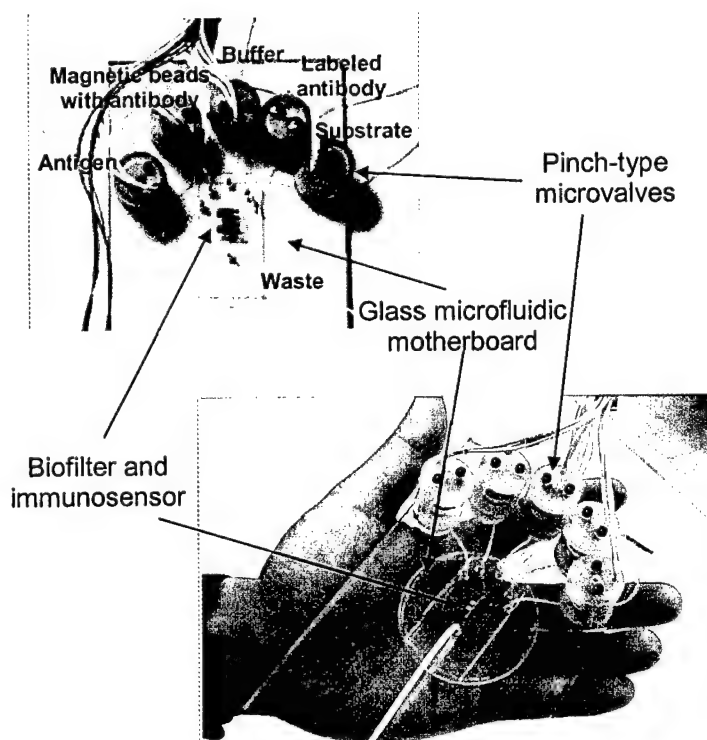
In summary, through this project we have successfully developed and characterized a portable integrated biochemical detection system using magnetic bead-based immunoassay, which has sampling and detection capabilities. The methodology and system, which has been developed in this project, can be applied not only to portable bio-warfare detection systems but also to generic bio-molecule detection and analysis systems by replacing antibody/antigen with appropriate bio receptors/reagents such as DNA fragments or oligonucleotides for the application to DNA analysis and/or high throughput protein analysis.



(a)



(b)



(c)

**Figure I-4: Developed microfluidic systems for magnetic bead-based biochemical detection**  
 (a) Automated microfluidic system; (b) Plastic based microfluidic system; and (c) Integrated microfluidic system on a glass motherboard.



## II. Problem Definition

As a research problem, we formulated the focus of our work on development of microfluidic components and systems, development of biochemical assays, and implementation of a compact electronics system.

### Microfluidic Components and Systems

In the realization of microfluidic components and systems, a large effort was given to development of desired microfluidic components using MEMS technology. The main problem was to understand fluidic behavior in microfluidic systems since objects in micro-scale follow different physical laws than in the macro world.

#### *Detailed problems include:*

- Development and improvement of magnetic microinductors to operate microvalves and biofilters
- Development of normally closed microvalves with no leakage and low power consumption since no microvalves suitable for the project were reported at the time
- Development of magnetic particle separators as biofilters that generate strong magnetic fields to capture and hold magnetic beads from flowing suspension at low power consumption
- Design and fabrication of electrochemical immunosensors with microelectrodes
- Optimization of the biofilter and biosensor structure to address an inherent conflict of the simultaneous requirement of rapid front-end throughput and fast response time
- Development of flow sensors to monitor flow rates
- Realization of a microfluidic system to control small amount of chemical or biological samples, providing selective sampling capabilities
- Integration of the developed microfluidic components on a microfluidic system
- Development of module-type generic systems, which can be combined on chip in a variety of ways to apply for various other fluid regulation systems
- Development of reliable and low temperature wafer-to-wafer and device-to-wafer bonding technology
- Development of microfluidic interconnection technology with minimal dead volumes

### Biochemical Assays

We determined that the electrochemical immunoassay as constituted with the magnetic microbeads is a proven technology that is applicable for developmental completion to project requirements.



***Detailed problem includes:***

- Detecting and identifying more than one analyte simultaneously in the highly foreshortened timeframe required by the mission
- Having a detection system which operates optimally for all four different analyte types (molecule, virus, spore and bacterium)
- Accounting for non-ideal properties of magnetic microbeads including inappropriate adhesiveness and some magnetic and transport properties
- Non-specific adsorption of biochemical components with the assay and microchannels leading to unwanted signal interferences
- Solution instability of the chosen enzymatic substrate chemical
- Possible fouling of the detector electrodes by components of the liquids within the microfluidics

## **Electronic Control and Analysis System**

Setting system specifications was a significant part of the research and was something that depended on the other groups as their parts of the research progressed. Although it would have been the ideal situation, we decided early on that it would be impractical to design an IC capable of even part of the system operation when the specifications would be changing frequently. So the individual board approach was chosen and assignments were made to different graduate students. That allowed the flexibility that was needed in a research project that was undefined insofar as the details were concerned.

***Detailed problems include:***

- Development of controller containing both a digital and an analog sub-system
- Development of specialized sequencer which can be externally programmed to accommodate different liquids and the varied sequences needed for microvalves/pumps actuation and control
- Providing and sequencing microvalve currents of hundreds of mA
- Measurement of nA range signal from the electrochemical immunosensor
- Battery operation
- Compactness

### III. Approaches

As stated, the main objective of the project was to develop a generic microfluidic system for biochemical detection. Therefore we divided the project into three research areas: (1) MEMS components and microfluidic systems, (2) biochemistry and electrochemical detection, and (3) electronic circuitry and control systems. Each task is closely related to each other and extensive collaboration was enforced to overcome any problems encountered. Approaches we have used to reach the project goals are described below.

#### MEMS Components and Microfluidic Systems

In realization of the proposed microfluidic biochemical detection system, development of microfluidic components and systems are essential. At the beginning of the project, we decided to attack the goal in mainly two parallel approaches: (a) Meso/automated systems and (b) Microfabricated systems to avoid risks and to compensate any possible disadvantages.

#### Meso/Automated Components and Systems Approach

##### Meso System with Standard Components

First we developed a meso system to demonstrate a system concept as shown in Figure III-1 in collaboration with Tekmar-Dohrmann, our industrial partner on this project. The system consists of commercially available valves and conventional tubing. The purpose of the meso system was to benchmark the performance of the individual MEMS components against the standard components and quantitatively evaluate the enhancement in detection of bio organisms, using MEMS components with replaceable standard components and micro-controller based control system.

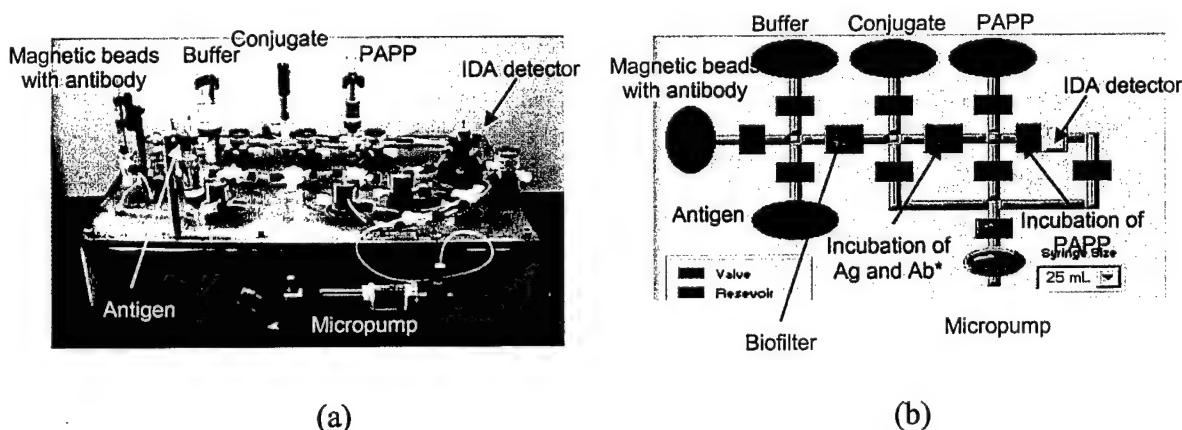


Figure III-1: (a) Realized meso-system, and (b) corresponding control software panel

### **Automated Microfluidic System**

We shrank the meso system into a hand-held system using newly developed microfluidic components such as microfluidic valves, pumps, magnetic curtain type biofilters, electrochemical immunosensors, and collapsible reservoirs.

#### **Microfluidic Valves**

Pinch valves, which were made of biocompatible silicone tubing, used to direct and control the flow of the fluids. A commercially available mini solenoid was used to actuate the pinch valve, since MEMS actuators were not yet capable of supplying the required actuation force. The pinch force for one batch of valves were supplied by a "magnetic spring" as shown in Figure III-2, while for the other batch of valves, the pinch force was supplied by a "cricket like" spring as shown in Figure III-3. In the valve which uses the magnetic spring, two like poles of two permanent magnets were placed close enough so that the repulsive force between the poles pinch the silicone tube, closing the fluid passage. The membrane type valves have a silicone elastomer membrane to close and open the fluid path. All sets of valves were tested to be leak-tight up to 30 psi. The actuation current to open the valve was 80 mA at 5V.

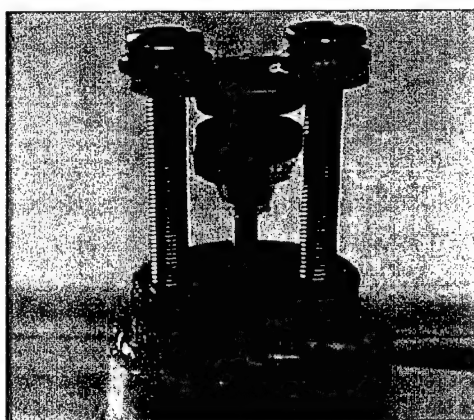


**Figure III-2: Valve with magnetic spring**



**Figure III-3: Valve with "cricket like" spring**

#### **Magnetic Curtain Magnetic Particle Separator**

A novel solenoidal "magnetic curtain" magnetic particle separator was used to capture the magnetic beads for chemical gestation during successive processing. The magnetic field is generated by a solenoidal coil along the fluid microchannel. When the field is actuated by the electromagnet, the field gradient on the two ends trap beads within the electromagnet. They will remain in place even as buffer and reagents are flown through this region. The problem is that when the electromagnet is actuated, beads cannot be moved into the system. Therefore we must open up the input end of the magnetic curtain using a critical combination of two nickel bars (wires or deposited nickel) and a stainless steel spoiler collar to distort the field. The nickel bars also allow an even

distribution of beads along the axis for effective biochemical gestation. When the electromagnet is deactivated by the programmed electronic control system, the beads move out with the flow.

A capture efficiency of more than 99% was achieved for a current of 42 mA at 12 V. The magnetic beads were uniformly distributed along the magnetic field lines in the magnetic curtain region. The "magnetic curtain" magnetic particle separator is shown in Figure III-4. The device is a solenoid with an axis running parallel to the flow channel so that the external gradient at the edged trap the beads. The fact that the beads seen "float" within the magnetic curtain, allows for more effective chemical processing because all surfaces are exposed to the fluid. This magnetic separator can easily be adapted to a purely MEMS configuration, although the present model consists of magnet wire wrapped around the channel or tube.

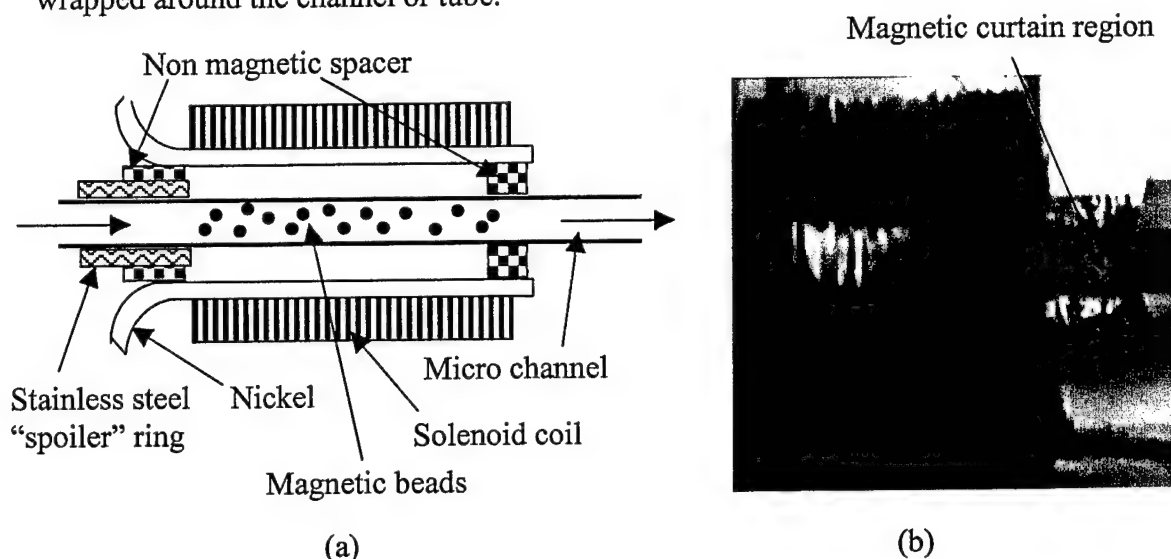


**Figure III-4: Magnetic Separator**

(a) Schematic illustration and (b) photograph of the magnetic curtain magnetic particle separator.

#### Micro Wire Electrode and Micromachined IDA

Both a micro wire electrode flow cell and a micromachined inter digitated array (IDA) were used for electro chemical detection as shown in Figure III-5 and Figure III-6, respectively. The wire electrode was fabricated using 25  $\mu\text{m}$  gold wire as shown in Figure III-5.



**Figure III-5. Photograph of the micro wire electrode**

Two gold wires were placed adjacent to each other with a spacing of 25  $\mu\text{m}$  for the working electrodes and a third wire was placed with a spacing of 200  $\mu\text{m}$  for the auxiliary electrode. The reference electrode was made by coating a gold wire with a very thin layer of silver paint (which eliminated an earlier problem of the silver dissolving into the solution) and placed 50  $\mu\text{m}$  away from the working electrode. The lower level of detection of the micro wire electrode was measured to be in the range of  $10^{-7}$  M (molecular concentration) with para-aminophenol (PAP). The micromachined interdigitated array (IDA) electrode gives increased sensitivity but is more fragile.

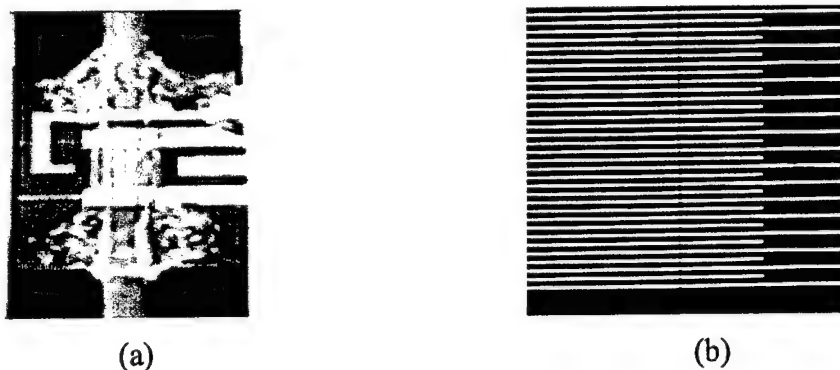
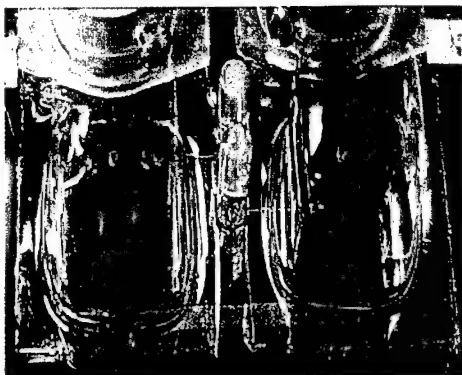


Figure III-6. Microphotograph of the micromachined IDA

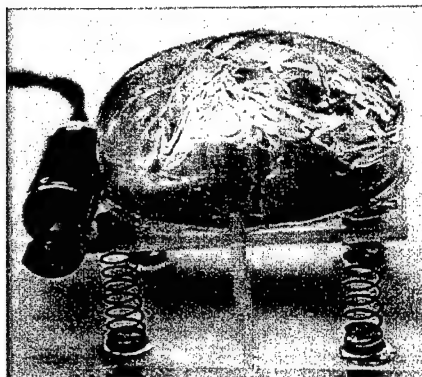
(a) Packaged IDA and (b) IDA fingers.

#### **Collapsible Polyethylene/Teflon Reservoirs with Stirrer**

The collapsible polyethylene/Teflon<sup>TM</sup> reservoirs with a magnetic bead stirrer (to prevent beads settling down due to gravity) as shown in Figure III-7, were used to store the fluids on the system. These were fabricated by using a wax sacrificial layer technique. A carrier buffer, surface modified magnetic beads, secondary antibody and the substrate were stored in the four collapsible polyethylene/Teflon<sup>TM</sup> reservoirs. In Figure III-7 a miniature motor with off-center mass is used to prevent bead settling down, however a piezoelectric actuator was also successfully used. The polyethylene reservoir can easily be scaled up or down (one is quite large at approximately 4 cc), as the Teflon reservoirs.



(a)



(b)

**Figure III-7. Polyethylene/Teflon reservoirs with stirrer**

(a) Teflon reservoirs and (b) Polyethylene reservoir with stirrer

### **Valveless Mini Rotary Pump**

A valveless mini rotary pump was used to pull the fluids through the system in this version, as shown in Figure III-8. The rate of pumping can be varied from a few nl/minute up to 1 ml/minute and the power consumption of the pump is 3 mW at the highest rate of pumping. The cogged wheel squeezes fluid through a 500  $\mu\text{m}$  tube or integrated silicone substrate. Again, the system can be scaled to a much smaller size.

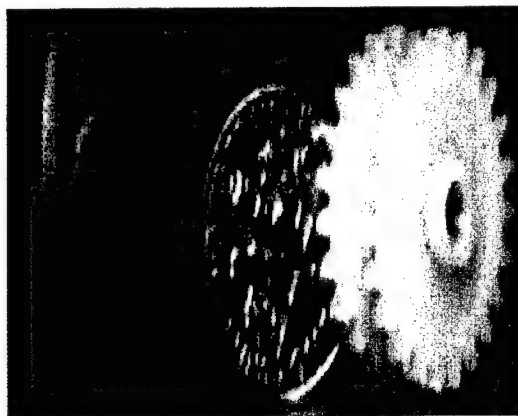


**Figure III-8. Photograph of the valveless mini rotary pump**

### **System Integration and Results**

Realization of the automated integrated microfluidic system, using the previously described components and the immunoassay results obtained with this system will be discussed in Section 1 of Chapter VI.

### **Micro Flow Sensor**

To monitor the microfluidic system and to apply feedback into the controller, a micro flow sensor was investigated and developed. The micro flow sensor operates not

unlike a hot wire anemometer. The input current applied to the sensor heats the sensing element above the ambient temperature to a steady state temperature, which depends on the velocity of the liquid in the microchannel. Ultimately, a thermal boundary layer within the liquid flow field is developed, where the thermal boundary layer thickness depends on the velocity and the applied input current. If the flow rate in the microchannel is kept constant, a velocity profile as shown in Figure III-9 is formed. The thermal boundary layer thickness can then be altered by varying the amplitude of the input current. With increasing input currents, the thermal boundary layer extends further into the liquid flow field. This can also be seen in Figure III-9. In essence, one can picture a "thermal dipole" that penetrates further into the microchannel, where higher velocities govern. These higher velocities convey more heat away from the sensing element, resulting in a higher sensitivity of the micro flow sensor.

Figure III-10 shows the relative change of the sensor output voltage as a function of flow rate for different input currents. The output voltage at 100  $\mu\text{l}/\text{min}$  with an input current of 3 mA, drops by 10.7% (1.4 V) from its zero flow value, whereas it only drops by 0.55% (14 mV) with an input current of 1 mA.

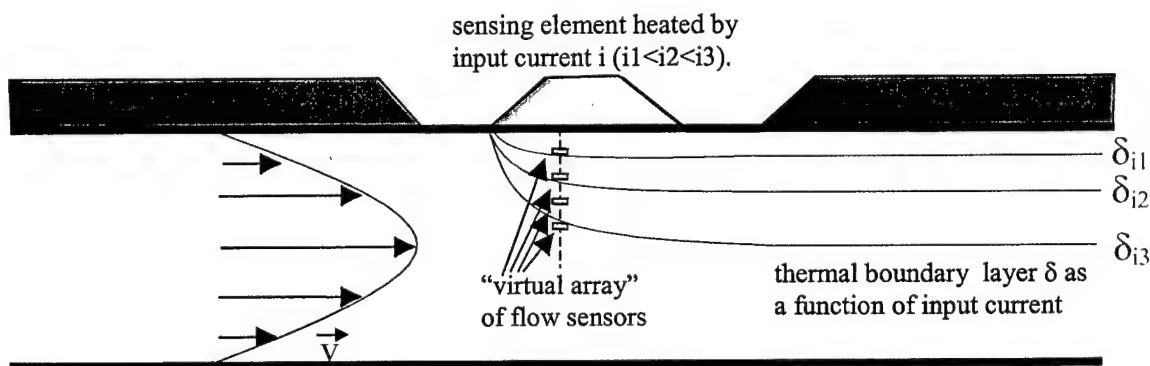


Figure III-9: Schematic of the micro flow channel with indication of velocity profile, thermal boundary layer and virtual sensors

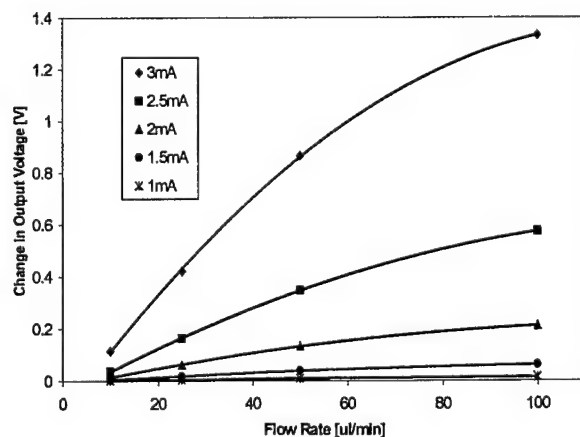


Figure III-10: Relative change of the sensor output voltage as a function of flow rate for different input currents

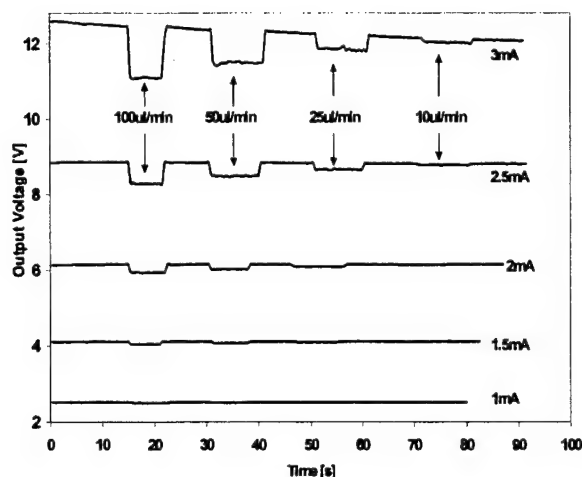


Figure III-11: Output voltage is plotted as a function of time for different input current levels and with varying flow rates

## Microfabricated Components and Systems Approach

Approaches to realize microfluidic biochemical detection systems were focused on development of novel microvalves, biofilters, immunosensors, and microfluidic motherboards at the early stage. Integration of these developed microfluidic components to construct microfluidic systems for biochemical detection was explored after development of all microfluidic components. A couple of new technologies, such as surface mountable bonding technique and microfluidic interconnection technique, were also explored for successful development of microfluidic components and integration of microfluidic systems.

### Biofilters and Immunosensors

Because the magnetic bead-based immunoassay was targeted as a proof-concept of a generic microfluidic biochemical detection system, magnetic particle separators (or biofilters) and electrochemical sensors were considered as key components. Magnetic beads are used as both substrate of antibodies and carriers of target antigens. A simple concept of magnetic bead-based bio-sampling with electromagnet for the case of sandwich immunoassay is described in Figure III-12. Antibody coated beads are introduced on the electromagnet and separated by applying magnetic fields. While holding the antibody-coated beads, antigens are injected into the channel. Only target antigens are immobilized and thus, separated onto the magnetic bead surface due to antibody/antigen reaction. Other antigens get washed out with the flow. Next, enzyme-labeled secondary antibodies are introduced and incubated, with the immobilized antigens. The chamber is, then, rinsed to remove all unbound secondary antibodies. Substrate solution, which will react with enzyme, is injected into the channel and the electrochemical detection is performed. Finally the magnetic beads are released to waste chamber and the biofilter is ready for another immunoassay.



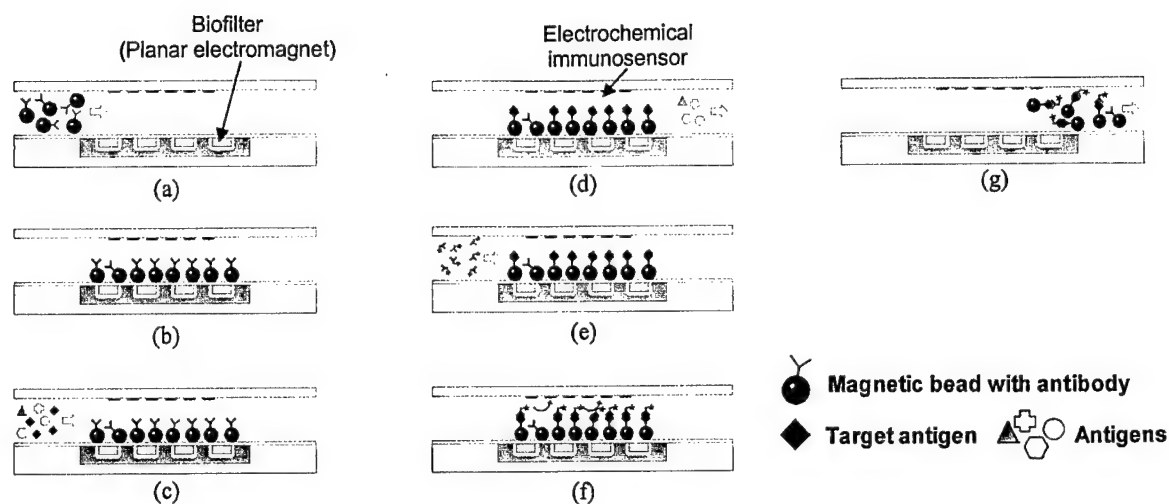


**Figure III-12: Conceptual illustration of bio-sampling and immunoassay procedure**

(a) injection of magnetic beads; (b) separation and holding of beads; (c) flowing samples; (d) immobilization of target antigen; (e) flowing labeled antibody; (f) electrochemical detection; and (g) washing out magnetic beads and ready for another immunoassay.

To achieve bio-sampling and biofiltering capabilities, biofilters were developed as shown in Figure III-13. Biofilters were designed to separate magnetic beads from fluid suspension and to hold the separated magnetic beads in fluid flow during bio-sampling procedure. An embedded serpentine inductor structure was suggested to maximize magnetic forces on a magnetic bead at a low current operating condition at the early stage of the project. However, we needed a biofilter, which produces much strong magnetic forces depending on dimension and structure of microfluidic channels. So we have also designed a new biofilter using magnetic interconnection technology as described in Figure III-14. External electromagnets give freedom to control the range of magnetic fields when a strong magnetic field is required.

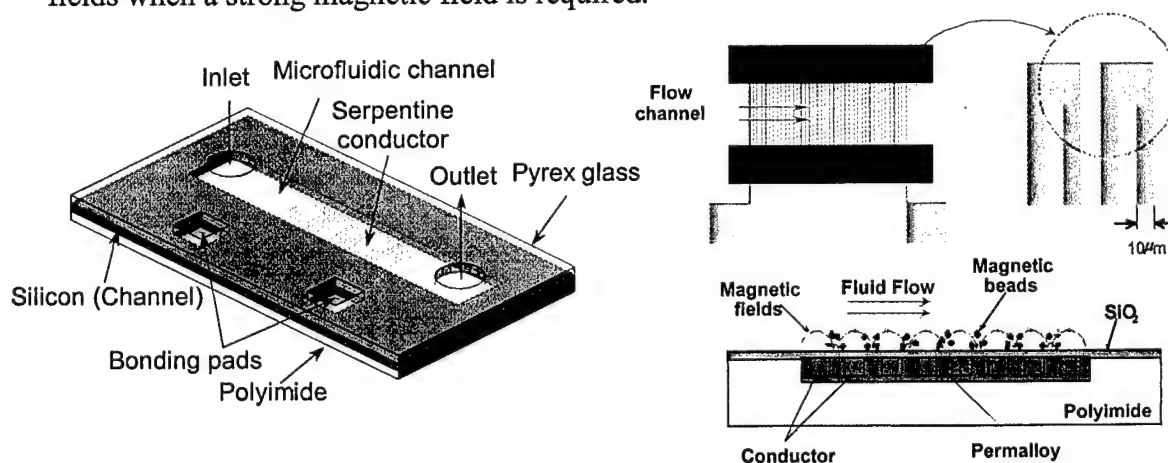


**Figure III-13: Schematic illustration of the designed biofilter with embedded serpentine inductor structure**

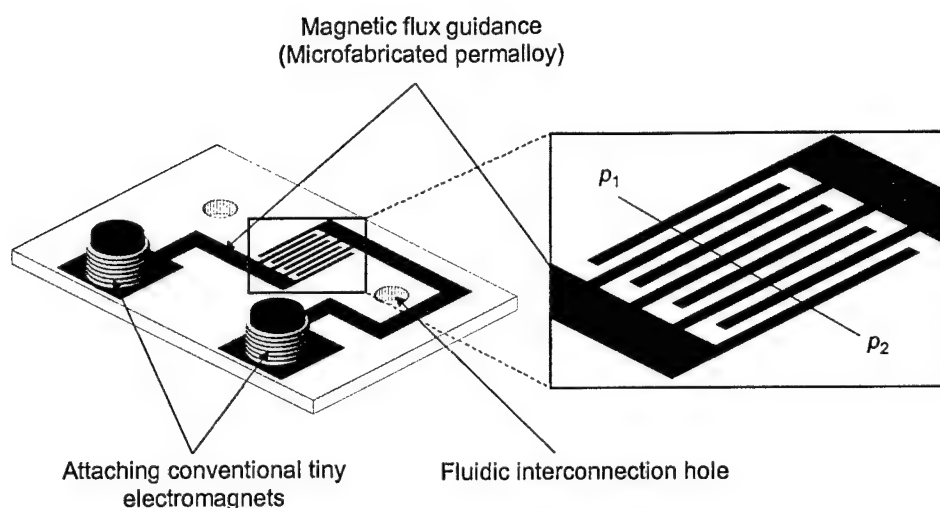


**Figure III-14 (a): Schematic illustration of the surface-mountable biofilter**  
(electroplated permalloy guides magnetic fields from the attached conventional tiny inductors).

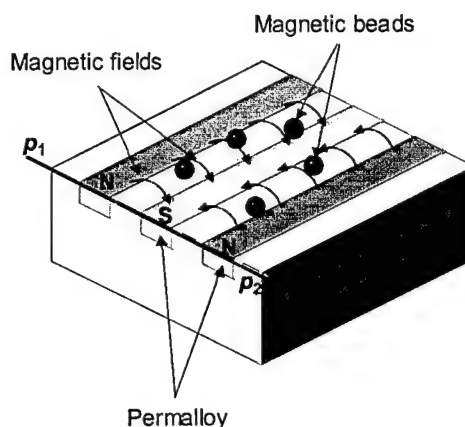


**Figure III-14 (b): Schematic illustration of the surface-mountable biofilter**

Interdigitated array (IDA) microelectrodes are particularly interesting because they are geometrically different from conventional electrodes and this results in particular electrochemical behavior. For this reason, electrochemical detection using IDA was selected in this project for biochemical detection of magnetic bead-based immunoassay. Figure III-15 describes the electrochemical detection principle and enzyme sets. Alkaline phosphatase (AP) and p-aminophenyl phosphate (PAPP) was chosen as enzyme and electrochemical substrate. Alkaline phosphatase make PAPP turn into its electrochemical product, p-aminophenol (PAP). By applying potential into microelectrodes, PAP gives electrons and turns into 4-quinoneimine (4QI), which is oxidant form of PAP.

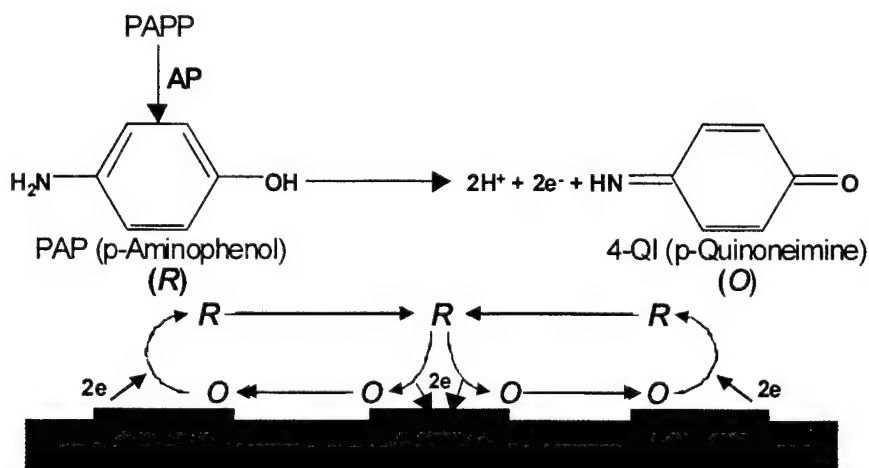
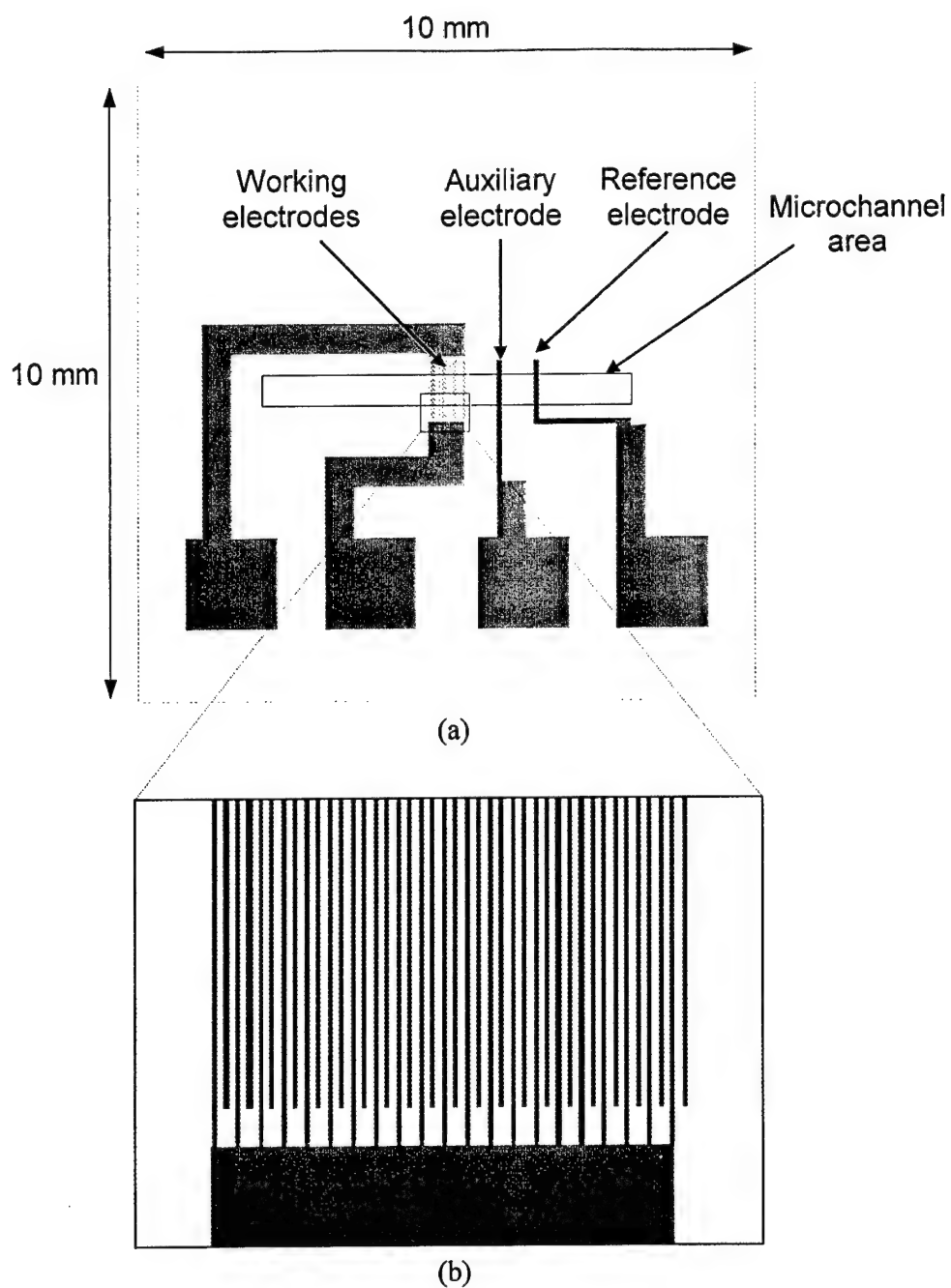


Figure III-15: Enzymatic kinetics for electrochemical detection of the immunosensor

Design and dimensions the electrochemical immunosensor are shown in Figure III-16. The reference electrode and auxiliary electrode are 100 mm wide. Interdigitated array electrodes are 7.5 mm wide and 7.5 mm spaced. Overall size is designed to fit the biofilter described above.



**Figure III-16: Design layout of the electrochemical immunosensor**

Dimension of reference electrode and auxiliary electrode is  $100\text{ }\mu\text{m}$  wide. Interdigitated array electrodes are  $7.5\text{ }\mu\text{m}$  wide and  $7.5\text{ }\mu\text{m}$  spaced.

The developed biofilter and electrochemical immunosensor were combined together and are shown in Figure III-17.

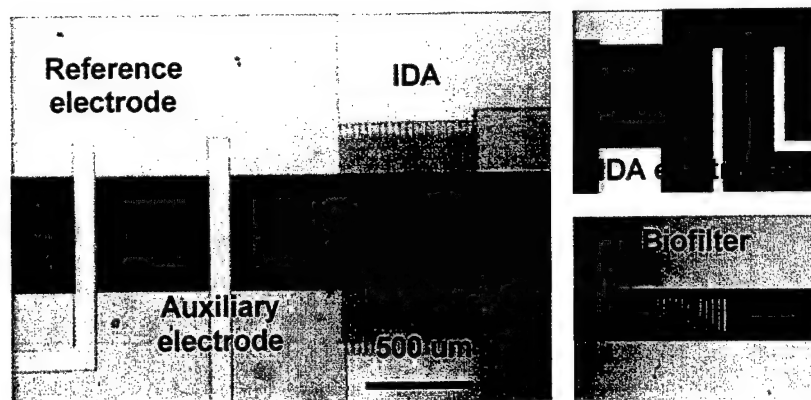


**Figure III-17: Microphotograph of the integrated biofilter and biosensor**

The volume of the fluidic chamber for biofiltration, reaction, and detection was calculated to 750 nl.

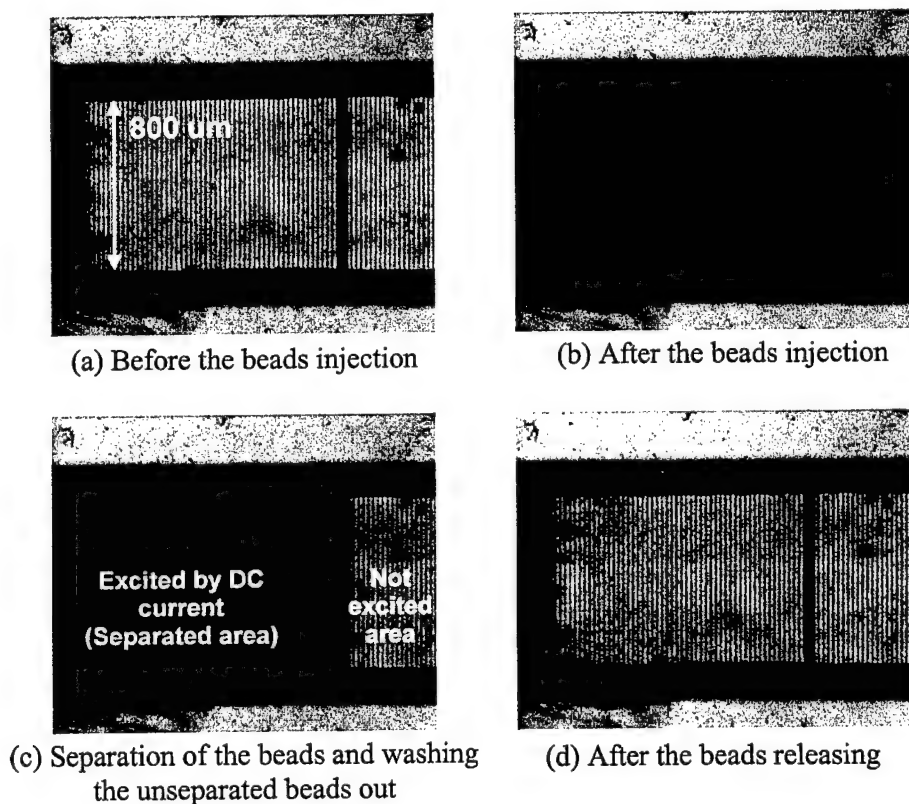
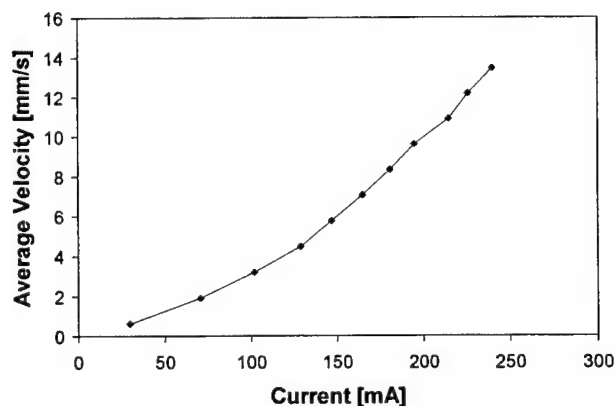


**Figure III-18: Separation test results**

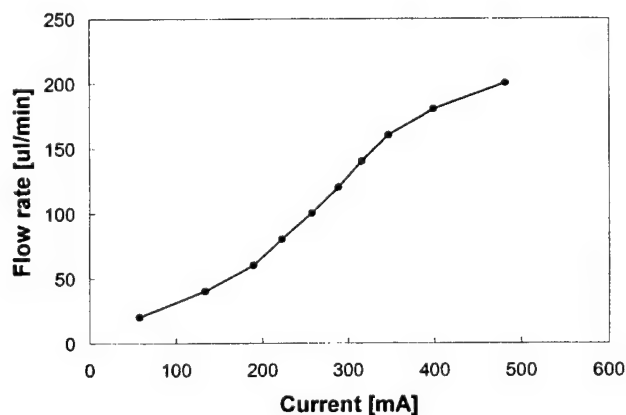
(a) before the bead injection; (b) after the bead injection; (c) separation and holding the beads; (d) releasing procedures, and (e) after complete release.

Fabricated biofilters and electrochemical immunosensors were fully characterized before integration. The fabricated biofilter was characterized in the following order to ensure its functionality in sampling and manipulating beads. First, the magnetic beads were injected into the microchannel. Next, the DC current was turned on. During separation, the unseparated beads were washed away with the fluid flow. After completely washing the unseparated beads out, the separated beads were released by turning off the applied DC current. All procedures were recorded through a microscope with VTR and major steps are shown in Figure III-18. The maximum average velocity at which the DC current holds the beads in the fluid flow has been also measured as shown in Figure III-19 for both biofilters.

The electrochemical immunosensor was also tested by flowing para-aminophenol (PAP), which is enzyme product, and the results are shown in Figure III-20.



(a)



(b)

**Figure III-19: Measured maximum fluid velocity and flow rate**

Beads are held over the electromagnet surface at various driving currents for the biofilters with (a) embedded serpentine inductor structure and (b) permalloy magnetic flux guides and external electromagnets.

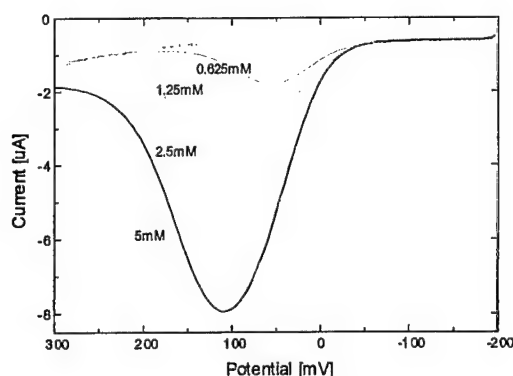


**Figure III-20: Calibration curve of the electrochemical immunosensor for different PAP concentration**

### **Microvalves**

To control flow sequences and amount of fluids for magnetic bead-based immunoassay, microvalves were also required even though development of microvalves were considered as one of the most difficult technologies in microfabrication. Since a magnetic actuation was implied to operate microvalves, development of magnetic microinductors was also emphasized based on UV-LIGA process in addition to both research on microfluidic behaviors and development of membrane type microvalves. Microfabrication steps for the microinductor are shown in Figures III-21 and III-22, respectively.

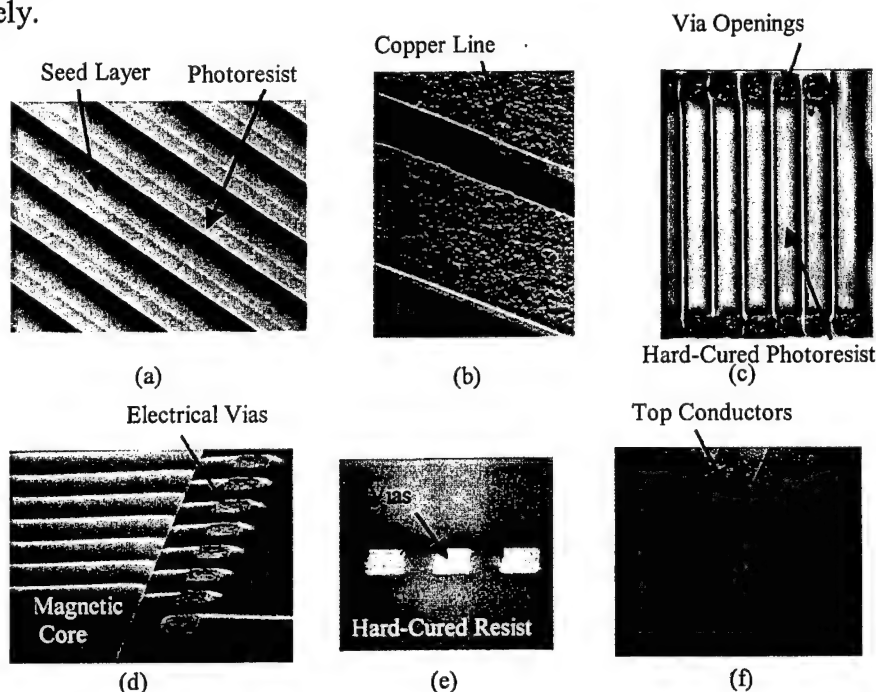


**Figure III-21: SEM photographs of micromachined solenoid-type inductors**

(a) initial photolithography; (b) electroplated copper lines which form the bottom conductors; (c) hard-cured photoresist that forms the first dielectric insulation layer; (d) electroplated magnetic core and electrical vias; (e) second layer of hard-cured photoresist; and (f) electroplated top conductor lines.

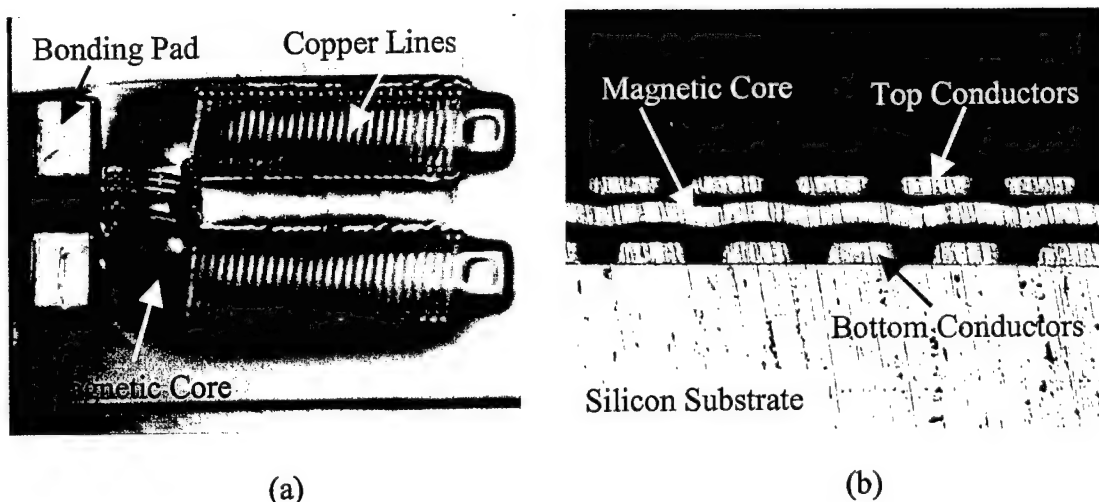


**Figure III-22: Photographs of fabricated solenoid-type inductor**

(a) Top-view of completed horseshoe-shaped electromagnet consisting of copper lines wrapped around a Ni/Fe magnetic core. Large copper bonding pads allow for easy electrical connection to the device. (b) Cut-view cross-sectional photograph of the same device. From this view, the three layers of the device can be clearly seen: bottom copper conductors, magnetic core, and top copper conductors. Each layer is separated from the next by an insulating dielectric.

To make normally-closed and leak-tight microvalves, rigid membrane materials have to be used to keep pushing the inlet in at any input pressure. However, this approach requires relatively large force to open the membrane up. Several versions of microvalves such as membrane-type, modified membrane-type with valve seats, and mesa membrane-type with valve seats, were developed as shown in Figure III-23.

At present, it is hard to find an ideal actuation mechanism for microvalves to achieve zero leakage and zero dead volume with lower power consumption, various pressure control capability, and fast response. Among other types of microvalves, pinch-type microvalves have been used for driving biofluids often because they can provide zero leakage flow, zero dead volume, fast response, high flow ranges, and easily replaceable tubing. There are few pinch-type microvalves available for biomedical microfluidic system applications. Although several models are commercially available, they are too large in size and not appropriate for surface mountable microfluidic systems. Furthermore, they require a huge amount of power consumption. To overcome these problems, a new pinch-type microvalve using a conventional tiny solenoid compliant with a surface mountable scheme on microfluidic systems has been also explored in addition to membrane-type microfabricated valves. A pinch microvalve for fluids connected with a conventional solenoid has been prototyped as shown in Figure III-24. A pinch microvalve includes a height-adjustable solenoid, a spring-loaded plunger, and a silicone tube. Due to the compressive spring force, the plunger pinches down the silicone tube, making this pinch microvalve normally closed. By actuating the solenoid, the plunger pinches off the tube, which opens the valve.



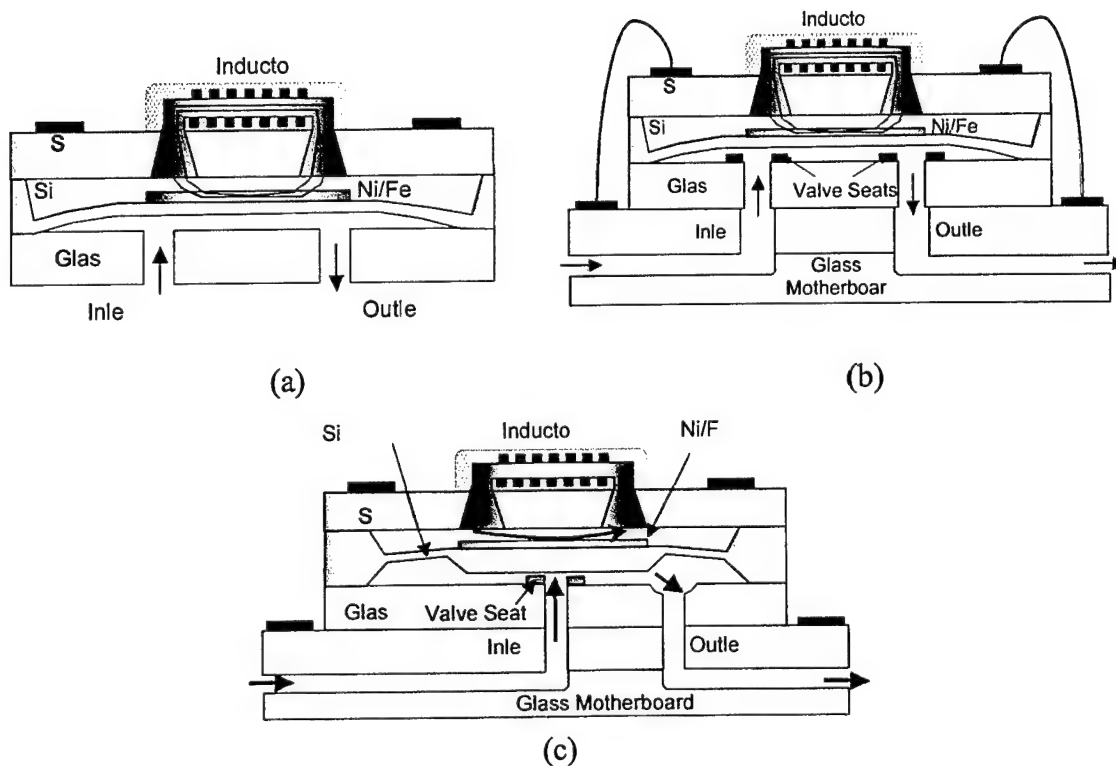


**Figure III-23: Several versions of microvalves using magnetic microinductors**

(a) Membrane-type magnetically actuated microvalve; (b) modified membrane-type with valve seats; and (c) mesa membrane-type with valve seats. All microvalves shown in the figure represent open state (actuated state).

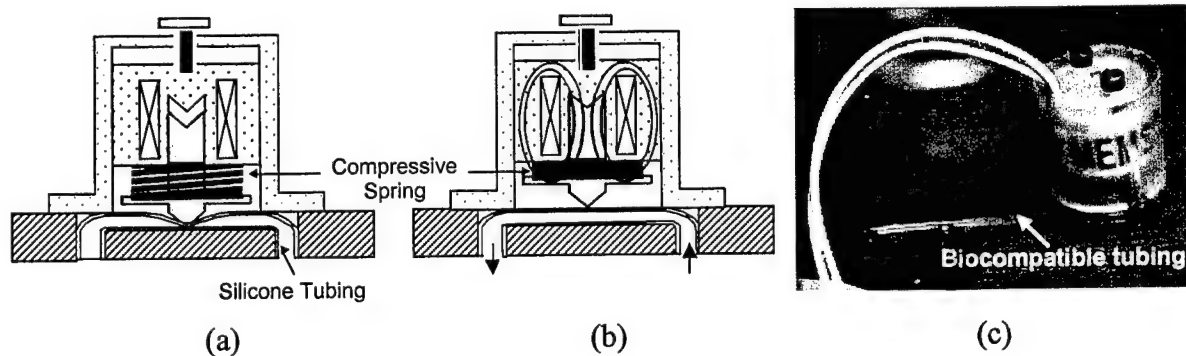


**Figure III-24: Pinch-type microvalve**

(a) closed position, (b) open position, and (c) photograph.

Upon completion of device fabrication, the performance of these microvalves was characterized using both nitrogen and DI water as the testing fluid. For both fluids, we

were able to measure the flow of fluid through the valve for various inlet pressures as a function of applied actuator current.

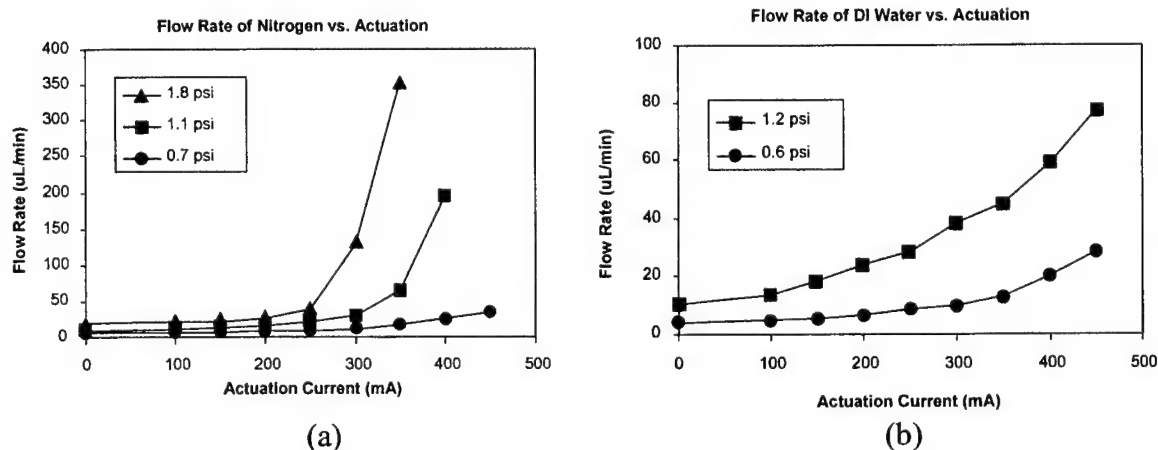


**Figure III-25: Measured flow rate of mesa membrane-type microvalves with valve seats**  
(a) nitrogen and (b) DI water as a function of actuation current for different inlet pressures.

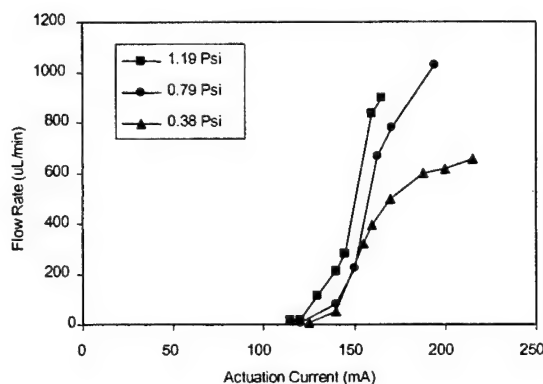


**Figure III-26: Experimental results of pinch-type microvalve**  
Flow rate of DI water as a function of the actuation current at various input pressures.

### Micropumps

With the same actuation principle as pinch-type microvalves, a pinch-type peristaltic micropump using serially lined three pinch-type microvalves and biomedical grade silicone tubing was also prototyped. The advantage of this type of pump is its ability to pump bi-directionally with almost zero dead volume. Furthermore, it has no leakage from one port to the other port at inactive state even when the fluid source has some pressure. There is no energy consumption to keep the fluid flow blocked, because the valves on this pump are normally-closed as shown in Figure III-27. Characteristics of the pinch micropump are shown in Figure III-28.

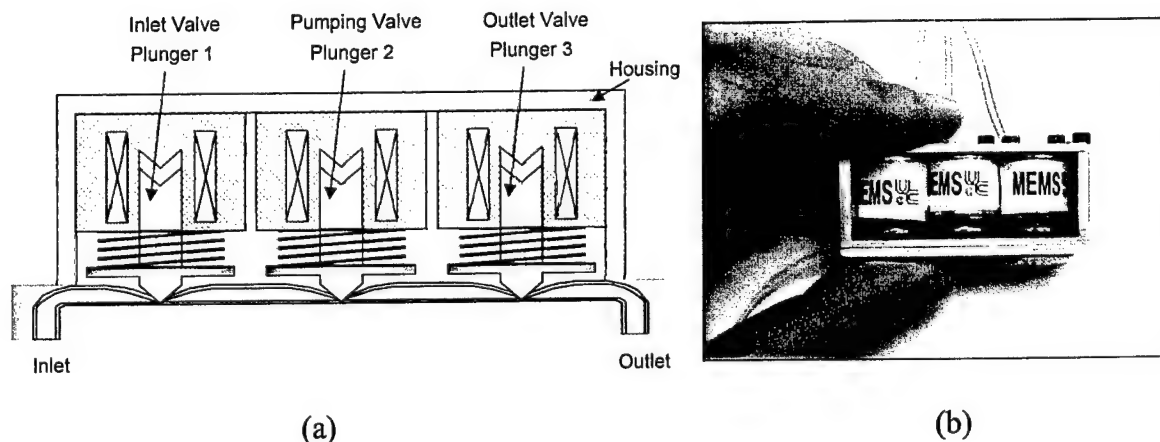


**Figure III-27: Surface mountable pinch-type micropump**

(a) Schematic illustration and (b) photograph of the fabricated micropump.

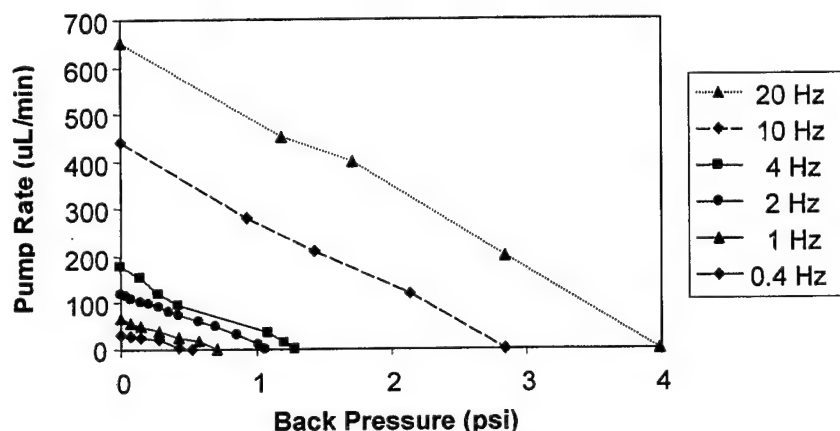


**Figure III-28: Pump rate as a function of back pressure with various driving frequencies**

### **Surface Mountable Bonding Technique**

One of the major limitations in the development of complete systems from individual components, was considered the inability to reliably bond the diverse and individual components, made of different materials such as silicon, glass and polymers, to other components or microfluidic motherboards at low temperatures. Figure III-29 shows a concept of surface mountable microfluidic system with fluidic components assembled on a fluidic motherboard. In implementing the fluidic systems, a reliable and repeatable bonding process requires that it does not alter the properties and performance of the components it is bonding. Therefore, a low temperature bonding process is

essential for ensuring the integrity of the components during bonding, packaging or assembling of these microfluidic components, because the low temperature reduces the detrimental effect of thermal mismatch and prevents degradation of metal and polymer structures of the microfluidic devices.

We used a bio-compatible spin-on Teflon-like material (CYTOP™, Asahi Glass Co.) as an intermediate bonding layer in the bonding of microfluidic devices on a fluidic motherboard at temperatures as low as 160 °C.

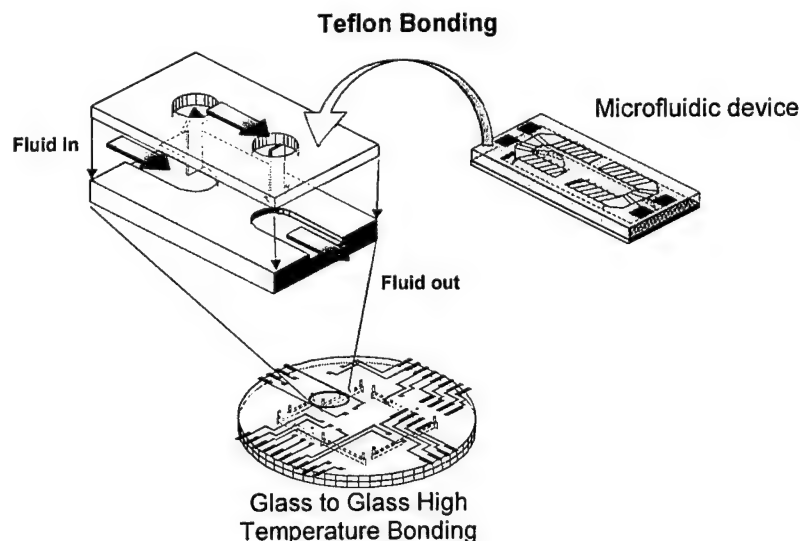
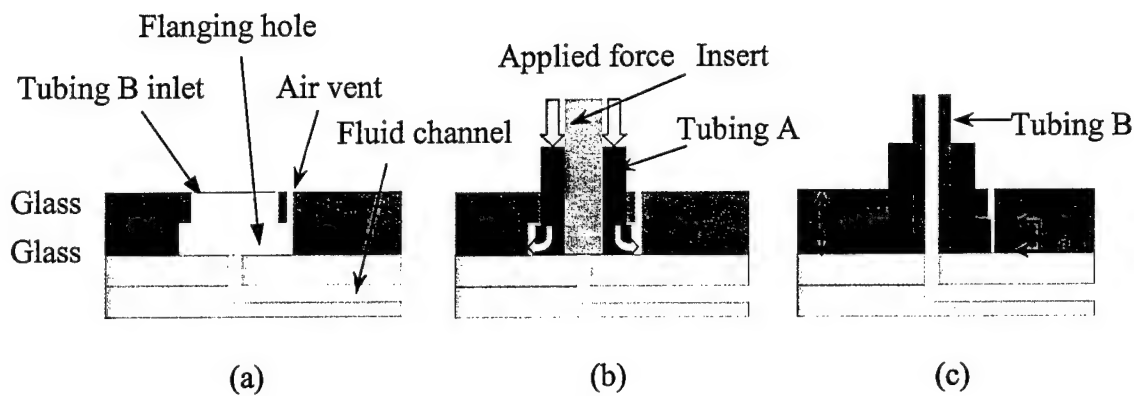


Figure III-29: Schematic illustration of the surface mounting technique on a fluidic motherboard

### **Microfluidic Interconnection Technique**

One of the challenges in the successful realization of a fully integrated system has been the development of reliable microfluidic interconnection technologies that allow for a fluidic connection to the “real world”. Certain parameters such as low dead volume, low-pressure drop, ease of fabrication, reliable and repeatable performance, and biocompatibility have to be met with stringent control for microfluidic interconnection schemes.

We developed and characterized a self-aligning fluidic interconnection technique, both resulting in very low dead volume and low-pressure drop across the interconnects. In developing the microfluidic interconnection scheme we have concentrated on achieving low dead volume, low pressure drop, high degree of biocompatibility and ease of fabrication technique. When a thermoplastic tubing (e.g., PEEK or TEFLON®) is heated at a transition temperature, it will soften and deformed outward filling up a larger hole in the so-called ‘flanging’ operation. If this process is performed in pressure controlled inlet or outlet fluidic holes, a self-aligning tube fitting can be easily achieved. This process is used to generate the fluidic interconnects as shown in Figure III-30. Microphotographs of the assembled interconnects are shown in Figure III-31.



**Figure III-30: Schematic diagram of serial interconnects**

(a) bonded glass wafer assembly; (b) flanging operation; and (c) assembled view.

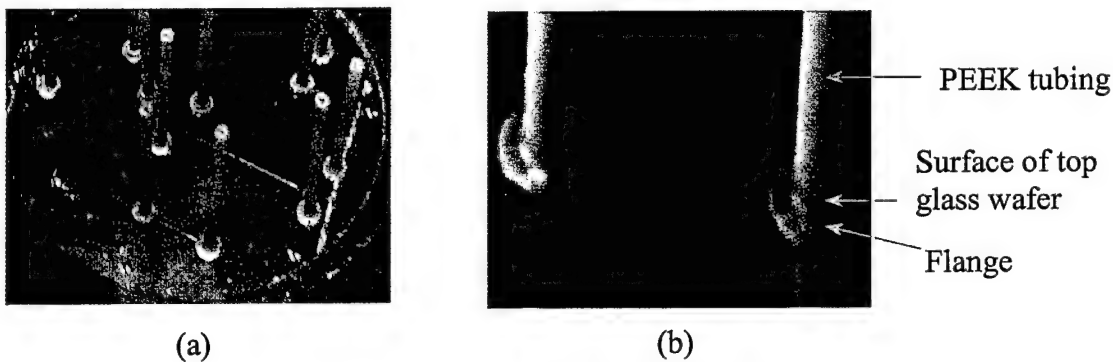


**Figure III-31: Microphotographs of serial interconnects**

(a) assembled view and (b) close-up of individual serial interconnect.

The interconnection scheme was tested for pressure drop and physical interconnect strength. For recording the pressure drop, the devices were connected to a syringe pump and a pressure sensor was connected in differential mode across the channel. While the flow rate was varied from 10  $\mu\text{l}/\text{min}$  to 500  $\mu\text{l}/\text{min}$ , pressure drops were measured. The results are shown in Table III-1 and Figure III-32.

As shown in Figure 5, the pressure drops shows a linear variation with flow rate. Furthermore, very low pressure drops are observed, which is desirable for the fluidic interconnects. The serial and parallel interconnects have virtually the same pressure drops, which indicates that good alignment has been achieved in both cases. The devices were connected to a high-pressure Nitrogen source to record the highest sustainable

pressure. To determine the pressure at which the interconnection failed, the devices were immersed in DI water. At the point of failure, bubbling was observed. Both schemes can withstand pressures in excess of 30 psi.

|  | Serial              | Parallel            |
|--|---------------------|---------------------|
| Flow rate ( $\mu\text{l}/\text{min}$ ) | Pressure drop (psi) | Pressure drop (psi) |
| 10                                     | 0.003               | 0.010               |
| 20                                     | 0.017               | 0.0244              |
| 40                                     | 0.50                | 0.057               |
| 60                                     | 0.079               | 0.086               |
| 80                                     | 0.11                | 0.12                |
| 100                                    | 0.14                | 0.15                |
| 200                                    | 0.31                | 0.31                |
| 300                                    | 0.47                | 0.48                |
| 400                                    | 0.64                | 0.65                |
| 500                                    | 0.81                | 0.82                |

**Table III-1:** Pressure drops for interconnects.

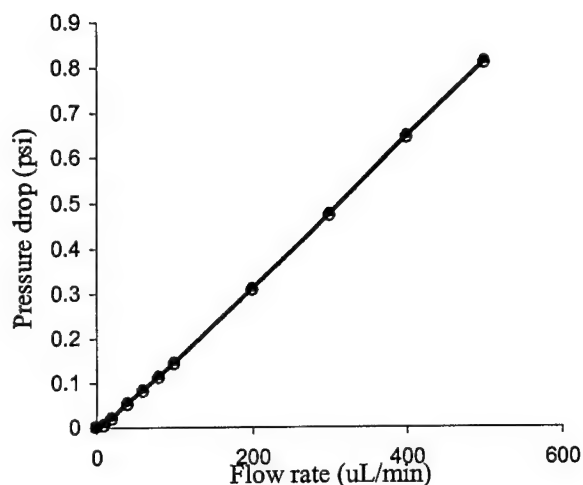


**Figure III-32:** Flow rate versus pressure drop

### **Microreservoirs**

In addition to microfabricated reservoirs, a commercially available miniature inflatable rubber bladder (refillable with hypodermic needle) was developed in a hybrid configuration with the microfluidic systems. Main advantage of this approach is ease of replacing the reservoirs upon demand of the system by plug in/out the reservoirs into the needles. Figure III-33 shows the developed microreservoir and Figure III-34 shows the mounted reservoir on the plastic based microfluidic system.

The pressurized reservoirs used for the plastic based system are made from an elastic silicone compound and sealed with PDMS (polydimethylsiloxane). The silicone reservoirs are commercially available and were purchased from Specialty Manufacturing

Inc. PDMS plugs were then cast in molds and their diameter corresponds exactly with the silicone reservoirs. PDMS exhibits a natural adhesion to the smooth silicone sleeve and the arrangement can seal low pressures (less than 2 psi) very well. Further, a rigid plastic sleeve was added around the reservoirs (with PDMS plug). The rigid plastic sleeve serves to compress the PDMS and the silicone reservoir thereby increasing the sealing capability of the reservoir. A fine gauge needle was used to introduce the fluid of interest in the reservoir. An excess of fluid introduced beyond the normal capacity of the reservoir ensured that the fluid was stored under pressure. The pressure can be varied by controlling the excess fluid volume introduced in the reservoirs. The reservoirs were then mounted on the plastic motherboard which had fine gauge needles, mounted on receptacles, where required. The needles punctured the PDMS layer and made contact with the fluid and upon opening the valves and pumping the fluid was introduced into the system without building any vacuum in the reservoirs.

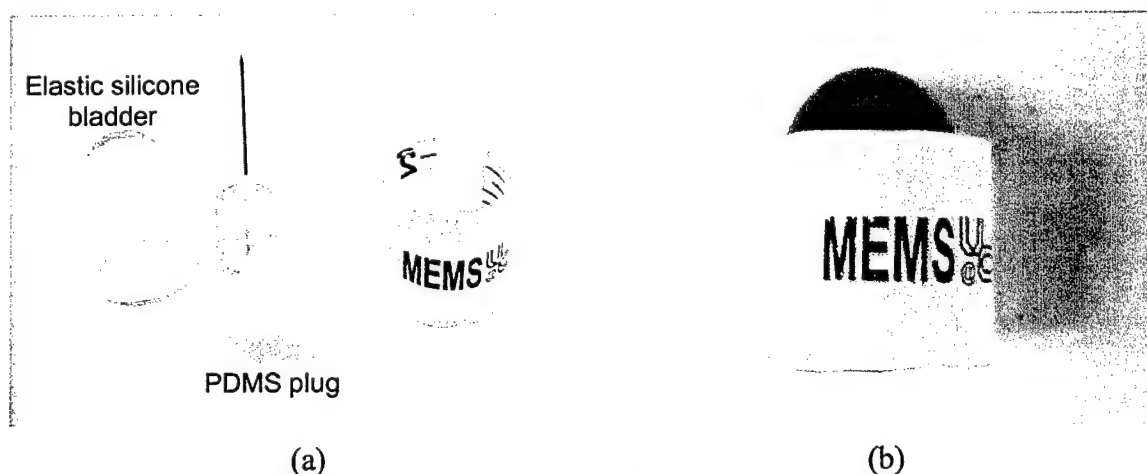


**Figure III-33: Developed reservoir using elastic silicone compound and sealed with PDMS**

(a) Pre-assembled reservoir and (b) Assembled reservoir with green fluid.

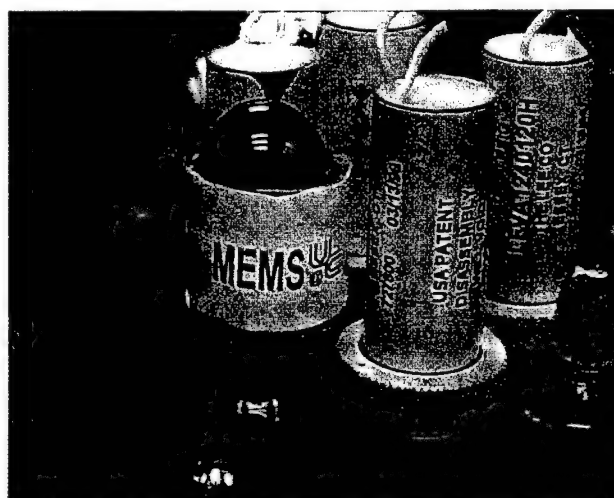


**Figure III-34: Reservoir mounted on the plastic based microfluidic system**

## Biochemistry and Electrochemical Detection

Our objective was to turn a molecular interaction phenomenon within a fluidic channel into a digital electrical signal. This involves both analyte concentration and signal development stages. Two major considerations were decided at an early point in the research. First, we were to assume some kind of fluidic input from an "unspecified" air collection stage. Second, we were to use a microbead matrix approach. With these considerations, we designed an electrochemical immunoassay system using microbeads for capturing the target particles. In this approach an antibody/enzyme conjugate is used for transducing the molecular recognition event into a proportional concentration of a dissolved chemical. The concentration of the chemical is then detected on an electrode within the fluid flow of the device. The electrode has a direct connection to the device electronics where the signal is immediately digitized, analyzed and exported.

### Details of the Approach

***The Magnetic Microspheres:*** The first stage in the device is the point where the liquid sample carrying the target particles enters the gadget and the target particles must be concentrated, segregated and otherwise treated for analysis. For this we add a quantity of antibody-coated magnetic microspheres into the fluidic stream. These microspheres are mixed with the target-laden inlet stream suspension and the targets are specifically bound to them. The type of microsphere used makes a significant difference in their properties and behavior in fluids, and their response to magnetic fields. The type we've used for most of our development has been the 2.8 micron diameter polystyrene/magnetite spherical particles from Dynal NA (Norway) known as Dynabeads as shown in Figure III-35.

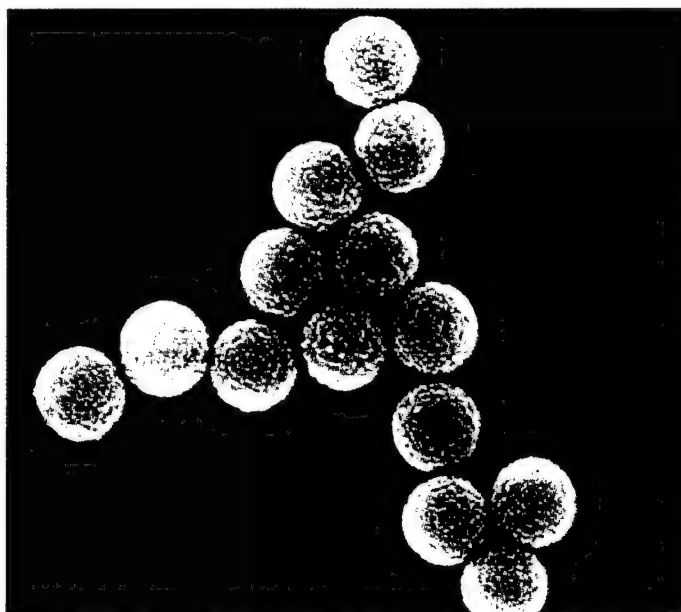


**Figure III-35: Magnetic beads**

(Dynabeads® M-280 Photograph was provided by Dynal Biotech Inc.). Diameter of the beads is 2.8  $\mu\text{m}$ .



These beads are comparable in size to a single bacterium such as *E. coli*. Among the mixture of unsorted particles in the fluidic stream, containing ten thousand, a million, or more types, only those bearing the specified molecular surfaces are recognized by the antibodies on the magnetic beads. They become attached, forming a magnetic particle/target complex in the stream. The specificity of the entire assay depends upon the antibodies coated on the beads. The beads may be kept in reservoirs within or outside of the device, to be chosen as conditions dictate. After use, the beads and fluidic liquids are disposed, but the device is reused so that the consumables, including the recognition surfaces, are separate from the device.

***Magnetic Handling of Target Complexes:*** Once the target particles are specifically tagged they are attracted to and held at an electromagnet in the flow path. All non-magnetic materials are swept away along the fluidic channel and excluded from the assay. The bead/target complexes may then be released by turning off the electromagnet and allowing them back into the fluid flow. In this way the target particles may be concentrated from irrelevant particles by a volume factor of a million-fold or more. Once captured, the bead/target complexes may be treated in place or released and recaptured downstream.

***Enzyme Tagging the Target Complexes:*** Once the bead/target complexes are separated from the inlet suspension they are mixed and treated with an enzyme/antibody conjugate solution. Antibodies that are specific to the target are chemically linked to the enzyme alkaline phosphatase (AP). The beads hold the target particles by means of an antibody and the AP-antibodies adhere to the target particles forming a sandwich with the target particles in the middle. In this way the target particles held by the beads are labeled with a proportionate amount of catalytic enzyme.

***Moving the Target Complexes to the Detector:*** Once the bead/target complexes are enzyme-labeled, they are washed and moved to the area of the detection electrodes. The washing removes non-bound enzyme conjugate. This non-bound conjugate would give a false positive signal and a high background, thereby raising the detection limit. By judiciously using flow switching and magnetic release and recapture, the washed bead/target/enzyme sandwich complexes are moved cleanly to the detection stage.

***Generating Detectable Chemicals:*** Within the fluidic chamber containing the detection electrodes the bead/target/enzyme complexes are recaptured from the fluid stream. The stream is switched and a substrate for the enzyme is introduced. This substrate is para-aminophenyl phosphate (PAPP) and it is not reactive to the detector. The AP enzyme catalytically breaks off the phosphate from the PAPP at a rate of hundreds to thousands per second per enzyme molecule. The product of the enzyme reaction is para-aminophenol, PAP, which is reactive to the detector. In this way the presence of each target, labeled with enzyme, is turned into very many reactive chemical signal molecules. A thousand-fold or higher amplification is achieved at this step.

***Detecting Generated Chemicals:*** The PAP generated by the catalytic enzyme tag is detected directly at an electrode adjacent to where the bead/target/enzyme complexes are held. This electrode is held at a voltage that removes two electrons from each PAP, yielding para-quinoneimine (PQI). Each electron removed generates a signal in the form of electrical current. This detector type is known as a potentiostat. Since the electrodes

are directly connected to, and driven by, the microelectronics running the entire device, the current signal is immediately converted into a digital information signal.

**The Entire Assay:** The magnetic bead-based electrochemical immunoassay we have developed has been run in several configurations entirely within the microfluidic platform. Detection of a protein target has been achieved with a 20 minutes cycle time. All the biochemical parts have been proven feasible.

### **Labeling the Magnetic Beads and Process Enhancements**

**Avidin Linkers:** We explored a number of chemistries to label the magnetic beads. One included applying a "modular" method of using the biochemical avidin-biotin linker molecules. The wide availability of biotinylated antibodies and the well-characterized chemistry of biotinylating antibodies made this an attractive method for easily changing the antibody specificity. We used commercial streptavidin-coated beads and explored the use of a charge-neutral type of avidin on our beads.

**Preformed Dendrimer Linkers:** In an effort to drive the antibody:target recognition process to a greater velocity/capacity/sensitivity we explored the use of these highly branched tree-like polymers as linkers between the beads and the avidin/antibodies. By using these spherical molecules, which are roughly half the size of the antibodies themselves, we attempted to 'roughen' the bead surfaces at the molecular scale and give the attached antibodies a greater reach and freedom to interact with their targets. We expected greater coverage of the bead surfaces by the antibodies resulting in a higher 'capturing' capability of the beads. A fivefold increased capacity of beads for carrying antibody was achieved with this linking method.

**Dendrimer Linkers Formed In Situ:** Several different approaches were explored for chemically synthesizing long-branched dendrimer linkers directly on the magnetic bead surfaces. These included polypeptide-based chemistry using lysine branching, polyamidoamine (PAMAM) dendrimer chemistry and tetrahydrofuran (THF) 'living polymer' synthetic approaches.

**Synthetic Simulants - The Bugbead:** The availability of biowarfare agent simulants, specifically the particulate ones, was a difficult practical issue. Although the harmless simulant organisms we obtained from the Aberdeen Proving Ground were useful in unitary device testing, their molecular definition and the ready availability of their associated antibodies was less than we had wanted. In order to create control analytes of less complexity and no viability we have invented and used our "Bugbead". This Bugbead is any of a number of beads that are chosen with specific properties and derivitized with surface antigens to approximate a particulate target in the micron size range. We have chosen beads with specific colors for easier microscopic tracking in assays and microfluidic channels. We have derivitized their surfaces with one, two, or more antigens in various ratios to explore their behavior in sandwich assays and multi-analyte or multi-antibody reactions. We have successfully created Bugbeads to react as a pathogenic organism (E. coli O157:H7) in commercial toxin and pathogen tests.

**Rapid Bead Immunoassay - the RDE Small Volume method:** Initial work with the 2.8 micron magnetic beads and their development in prototyping electrochemical immunoassays proved to be technically difficult at very low quantities. Early development using manual manipulation in microtiter plates and a flow injection detector required visible amounts of the beads - 25,000 beads at a time, about enough to cover a

printed period. A method was developed where a 40  $\mu\text{l}$  drop was trapped under a rotating disk electrode and a 4  $\mu\text{l}$  aliquot of bead slurry containing as few as 50 beads could be readily tested in a few minutes as shown in Figure III-36. This allowed rapid and sensitive exploration of microbead surface treatments for immunoassays.

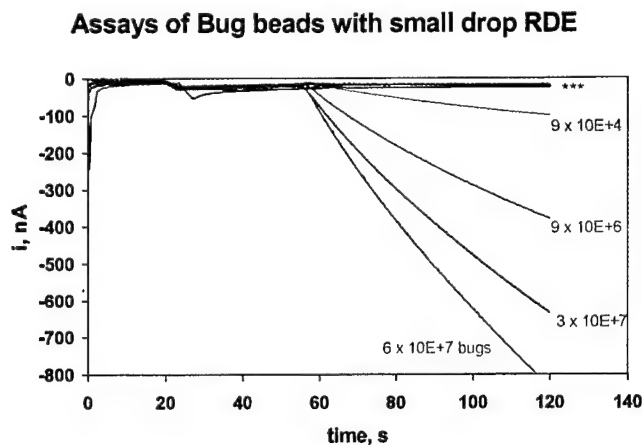


Figure III-36: RDE detection results

Minimum detected signal was observed in a solution of 9000 bugs / 50  $\mu\text{l}$  of which a sample of 2  $\mu\text{l}$  was assayed. The minimum detectable amount was estimated to be  $(9000 \times (40/50) \times 2) / 40 \sim 360$  bugs under these conditions.

**Visual Proof of Concept at the Nanometer Scale – the SECM:** The concept of doing an electrochemical immunoassay with microbeads was a new one when this project was initiated. A scanning electrochemical microscope (SECM) was used to test the reactivity of our microbead enzyme conjugate. A carbon fiber nanoelectrode was used to electrochemically scan a nanometer-resolution microscope stage upon which enzymatically-activated magnetic microbeads were immersed in a substrate solution. An electroactivity signal was generated as the nanoelectrode was scanned past aggregated bead structures and a visual representation of the electroactive product diffusing from the beads was evident. The instrument was used to test bead activities for various sized bead collections at surfaces.

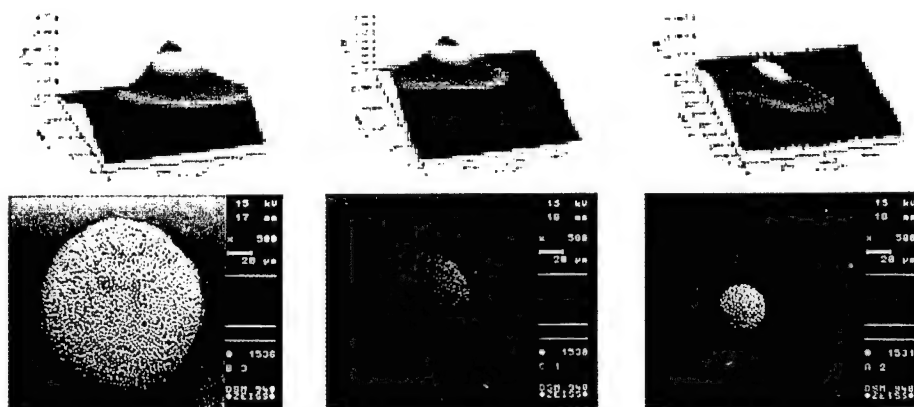


Figure III-37: Different immunomagnetic bead spots and corresponding SECM

**An Enhanced Detector - the IDA:** One way in which the potentiostat signal is increased is to convert the PQI back into PAP and allow the build-up of PQI and PAP to create larger current signals at a faster rate. By laying two sets of narrow strip electrodes in between each other and holding one at a voltage to take electrons from PAP and the other to return them to PQI, the reactants can cycle between the two, increasing the current signal at both. This is called an interdigitated array (IDA) with bipotentiostat cycling. The signal enhancement increases proportionally to the fourth power as the distance between the electrode strips decreases. Our on-chip fabricated IDAs that we have used have features of ~5 microns and give amplification factors of two to four. Some IDAs that we hoped to use have been fabricated with 1 micron and submicron features and give bipotentiostat cycling amplification factors of 400 or more.

## **Electronic Circuitry and Control Systems**

The electronic systems were the control, data capture and analysis aspects of the research. The research tasks in this area were divided into three main areas, namely that of valve and sequencing control, data gathering with system integration and display of results. Because of the interaction with our industrial partner and because of the desire to meet several different types of needs, a total of three fundamentally different systems were designed for the meso-scale system, the mini components/system, and the integrated microfabricated fluidic components/system. All electronic systems were tested using computer interface for data capture, analysis and display.

### **Microcontroller Based Integration**

A Motorola 68HC11 micro-controller board was obtained from Tekmar-Dohrmann Corp. The microcontroller provided a computational platform from which to support the MEMS control circuitry. This allowed complex timing, data storage, and waveform generation to be realizable without the need for an attached computer. The  $\mu$ C system initiated the movement towards a self-contained, hand held device. For the work reported,  $\mu$ C software was developed to control the data acquisition I/O interface. This software was implemented using ANSI C. The microcontroller communicates with this host PC through the serial peripheral interface (SPI). Data is transmitted/received from the microcontroller through this SPI. This microcontroller has various registers that are used for input/ output operations. Figure III-38 shows the block diagram of the system.

The microcontroller is connected to a FPGA to enable the serial transmission of data. The first level of circuitry involves the driver boards which supplies the pumps/valves with the necessary current. These driver boards supply up to 1000 mA of current. The driver board essentially consists of FETs where the load is connected to the drain of the transistor. This FET acts as a switch with its control signal being supplied by the gate. The gate control signal comes from the FPGA. The FPGA can be programmed according to the sequence to make the necessary valve turn on/off by addressing the particular latch and driving the necessary signal. In a similar fashion all the valves can be programmed through the driver board. The other main board of this system is the potentiostat board, which is mainly used to control the voltages at the IDA (Inter Digitated Array electrode) and to measure the current of the sample. The FPGA provides control signals for the current transducer multiplexers. These signals are used to latch the

multiplexers in this potentiostat board that in turn provides the necessary gain for the low-level analog signals. The voltages obtained in the electrode terminals are then given to the level shifter board that interfaces to the system ADC/DAC. The ADC/DAC board is used to enable the digital to analog conversion and vice versa. There are 4 ADC channels and 4 DAC channels.

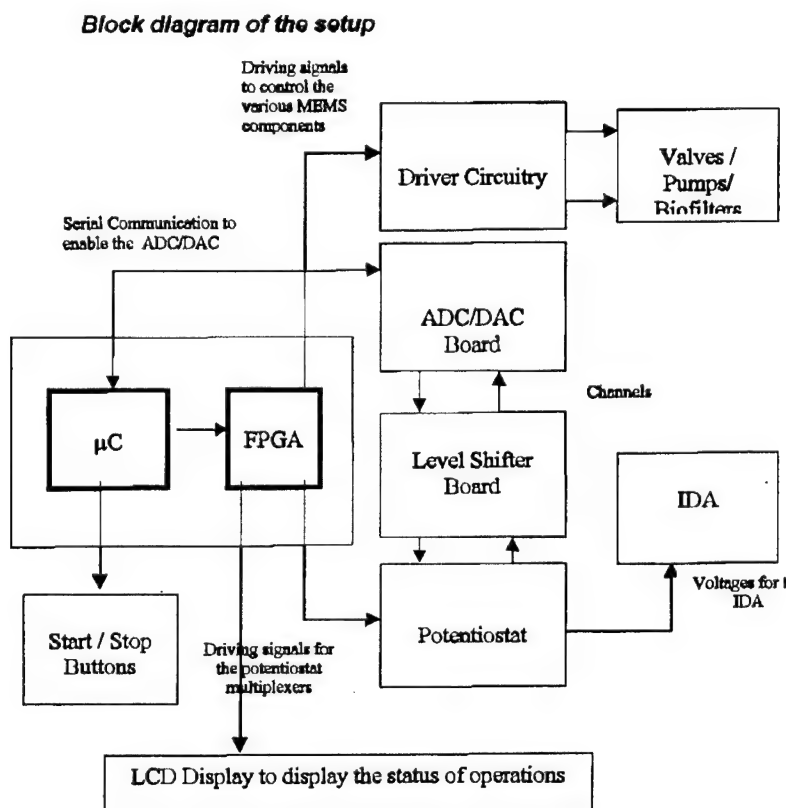
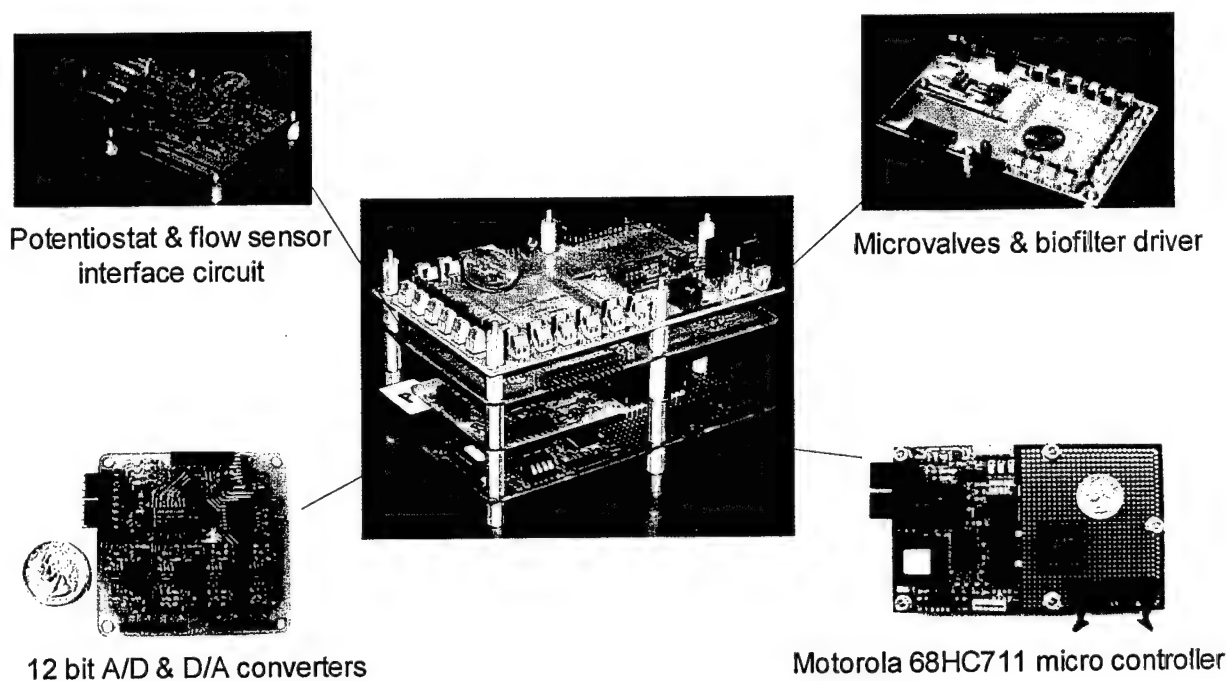


Figure III-38: Block diagram of the microcontroller based electronic system

There are a few hardware control buttons, mainly the Start, Stop and a Pause button that control the entire sequencing and detection processes and these buttons are interfaced through the FPGA. As the name suggests, the Start button starts the assay and if the sequencing has to be stopped in between for any errors, a Pause button is used which resumes the sequencing at the point where it was paused. There is also an LCD display driven by the FPGA that displays the status of operations going on at any particular instant of time. This LCD is connected outside of the stack. The LCD used is a 2 line by 20 character display which can be programmed in C. The control lines are the enable, register select and some data lines that are programmed to get the desired string displayed on the screen. The sequencing operation message is displayed on the LCD before the start of every operation so that the person viewing it can have a good idea of the status of the operations going on. This is the most general setup for any microfluidic system. This system can be modified according to the functionality desired. For example in the commercial microvalves, there is a considerable variation in coil resistance from device to device, due to factors during fabrication. The coils have resistances in the order

of ohms. Deviations of even a few ohms cause huge percentage changes in the total resistance of the device. The resistance also increases to a different extent when the device is bonded onto the motherboard of a microfluidic system. Hence, unlike a macro valve, a MEMS based one cannot be switched by simply using a FET as a switch between the element and the power supply. A constant current driver is required to provide a fixed current to these devices, whatever their resistances may be.



**Figure III-39: Stacked microcontroller based electronic system**

All boards have a uniform size of 3.5" x 5.5".

### **ADC/DAC Integration**

To properly support the chemistry, data needs to be measured and stored for computation, and analog waveforms must be generated. These waveforms create control voltages for the IDA and the MEMS flow sensor. High accuracy digital-to-analog (D/A) and analog-to-digital (A/D) converters were necessary for precise signal sampling and generation. To provide a smooth transition to using a  $\mu$ C based system, independent of a computer, the design required the capability to serially communicate with the  $\mu$ C (via SPI-Serial Peripheral Interface). In order to accommodate multiple MEMS devices, the devices must support several channels of I/O. The ADC/DAC board has 4 single ended A/D inputs and 4 single ended D/A outputs.



### **Level Shifter Circuitry**

The inputs from the ADC/DAC board are single ended. The potentiostat needs bipolar inputs for performing its operation. To achieve these bipolar inputs, the use of a level shifter is necessary. This level shifting board gets the inputs from the ADC/DAC board and converts them into bipolar inputs suitable for the potentiostat.

### **Display**

A two line 20 character LCD display is used to display the status of operations going on in the system. This is outside the stack and this gives an indication of the operations in progress at any instant of time. The display has an enable line and the data gets transferred on every falling edge of the enable. The R/W of the LCD is permanently grounded, as there is no read operation necessary for this system. The register select line of the LCD is used to select between instructions and data. The initialization procedure of the LCD includes setting the font, the number of lines, the number of dots, clearing the cursor, incrementing the cursor to the right when writing, etc. When the initialization procedures are carried out, the register select is at logic 0. The actual data to be transferred is converted to ASCII format by the microcontroller and this is transferred character by character to the LCD. The Register Select line is high when the data is being transferred. The operation of the system can be broken into a number of sequences. A sequence consists of either opening a few valves along with some pumping action or using the biofilter to hold the beads, etc. The LCD displays the operations going on after every sequence.

### **Potentiostat Board**

The potentiostat board is used to control the potential of the IDA electrodes and to monitor the resultant current at these electrodes. It controls the difference between the reference electrode and the two working electrodes by changing the potential of the auxiliary. The potential of the two working electrodes is controlled such that oxidation occurs at one electrode and reduction occurs at the other, which allows for desired amplification due to product cycling. The input voltage to the potentiostat is basically the bipolar voltage from the level shifter circuit. The outputs of the potentiostat go to the level shifter board that in turn sends the data back to the A/D and then to the microcontroller, which is displayed on the LCD.

### **Programming Techniques**

The FPGA has different address latches that control the valves, pump, biofilters, etc. These latches are selected by the I/O select lines of the microcontroller. The I/O select lines select a range of addresses and the last three bits of the address lines are required to select a single address latch. Once the desired address latch is selected, the corresponding bits are assigned a high or a low according to what is needed. The high is generally a 5 V and a low is generally 0 V. This is in turn connected to the boards and thus acts like a switch that can be controlled by the microcontroller. The sequencing of the components is called as functions in C and after every function, the micro-controller checks for the Stop button. The button is checked by a polling mechanism. There is a display message after every sequence. The display messages are sent out as ASCII strings using a function for outputting each of the characters in the entire string.

### Sequencing and Detection Graphical User Interface

Once the sequences are completed, the concentration of the analyte has to be determined. Electrochemical detection is done as the final step. This detection is done with the potentiostat board, which is used to sense the current, which in turn is proportional to the analyte concentration. The detection process was initially controlled by a PC. A graphical user interface was developed for the detection purpose.

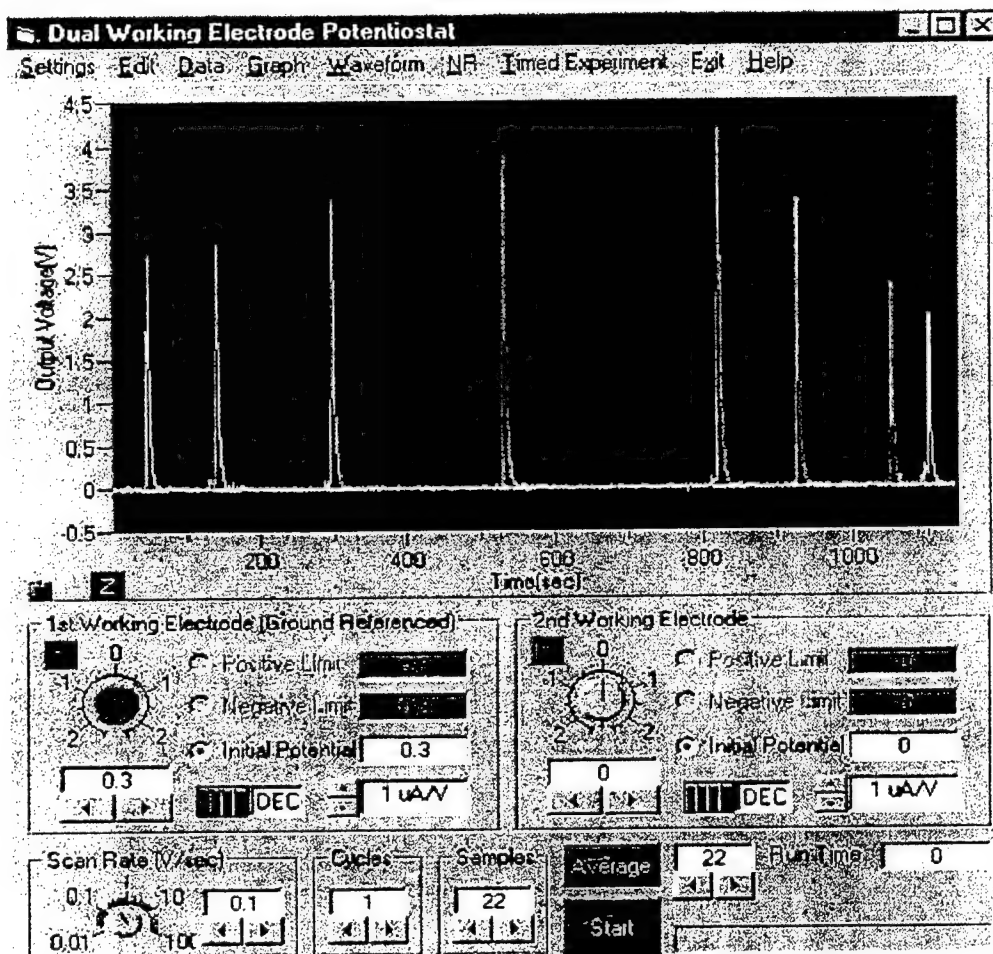


Figure III-40: Graphical user interface for biochemical detection

As shown in Figure III-40, there are various controls for the two working electrodes. The user may select a sine wave, square wave or triangle wave as the excitation waveform. In addition, the positive and negative limits of the waveform may be adjusted independently by the user. Once these values have been set, the user may select the initial phase of the waveform by varying the initial potential and by selecting whether the waveform begins by increasing or decreasing in magnitude. The second working electrode may also be adjusted in the same way. The scan rate is the rate of change in voltage that a working electrode may experience. By adjusting the scan rate



the user can control the frequency of the excitation waveform. The number of cycles refers to the number of iterations of the excitation waveform that will be generated. Finally, in the adjustable gain portion of the GUI, the user may individually select the gain setting resistors for the current-to-voltage converters of the working electrodes. In addition to these controls, the program allows the user to load and store the control settings, average the raw data over a specified number of cycles, save the raw or averaged data, plot the output waveform, or to export the raw or averaged data into a spreadsheet for further review. The graph gives an indication of the output voltage versus time. Offset correction schemes are also provided. The programming for the GUI was written in Visual Basic. In the microcontroller based system, since there was no provision of a computer, the data obtained from the assay was displayed on the LCD and stored as an array and then calibration curves were drawn based on the data obtained.

## IV. Problems Encountered

While performing the project various expected/unexpected problems have been encountered. Encounter problems have been solved except few specific problems and they made us to slightly modify some system specifications.

### Microfluidic Components and Systems

#### Air Trapping in Microfluidic Systems

Major problems came from our lack of knowledge on microfluidics as expected. Fluidic behavior in micro world does not come up to that in macro world. Pressure drops of the fluid were extremely large in microfluidic channels. Besides, surface tension becomes significant in microfluidics compare to "macro" fluidics, in which surface tension is usually ignored. Once air bubbles are trapped inside of the microfluidic channels, we could hardly take it out of the microfluidic systems because the trapped air bubble generates enormous pressure drops if it is trapped bending point of microfluidic channels. Two possible solutions were explored that 1) purging the microfluidic channels with vacuum helped to prevent air trapping when we inject sample fluids and 2) minimizing bending point of microfluidic channels reduced the probability of air trapping.

#### Integration of the Microfluidic Components to the Microfluidic Motherboard

We continuously failed to test fully integrated microfluidic systems because of almost same problems listed above. After a couple of trials and errors, we found that misalignment of inlet/outlet holes are occurred during the bonding process of the microfluidic components to the microfluidic motherboards. There were two reasons of misalignment of inlet/outlet holes: 1) we made inlet/outlet holes by mechanical manual drilling so the position of the holes were not accurate; and 2) we had to apply a certain mass on a microfluidic component during bonding process and consequently slight movement of the microfluidic device caused mismatch of the holes. We have solved these problems by giving enough margins to the holes and by using *Karl Suss* bonder which was purchased as part of this project.

#### Membrane-Type Microvalves

Microfabricated microvalves are a most challenging task in the MEMS community. We were optimistic in the development of membrane-type magnetically driven microvalves since we were very experienced in fabricating magnetic microinductors. What we encountered in the project was not so optimistic. We designed and developed three different models of membrane-type microvalves but the performances of the microvalves were not satisfactory. For gases such as nitrogen, the microvalves showed relatively good results and performances – no leakage and normally closed – but for liquids, there was a leakage problem and an air-trapping problem. Once the liquid-air interface passes the membrane structure, the valve lost its function. Even though there was no trapped air bubble, long term operation caused air generation from liquids by possible heat accumulation, dissolved air in liquids, and material stress in silicon/permalloy. We tried to solve these problems by modifying electromagnets to reduce heat generation, purging inert gases into the microchannels, and adopting mesa

membrane structure. All of the trials helped a lot but the operation was still not perfect. Hence we have concurrently developed a few different microfluidic systems such as the automated integrated microfluidic system, which has locally fabricated pinch valves using a commercial actuator for valve actuation, and the plastic microfluidic system with commercial microvalves as a parallel back-up system. Still we couldn't abandon the fully integrated microfluidic system so eventually we developed surface-mountable pinch type microvalves to overcome any difficulties. The surface-mountable pinch type microvalves showed almost zero dead volume in addition to reliable and functional operation – no leakage and normally closed mode – for biochemical analysis application.

### **Clogging of Magnetic Beads**

We expected there might be a clogging problem of magnetic beads at dead volume area and/or certain microstructures like membrane-type microvalves. Therefore design and development of a planar magnetic particle separator and biofilter was much concentrated. However, more significant clogging occurred on surface of a plane microchannel due to “suspicious” surface energy of materials. So we tried to use silica tubings for the automated integrated microfluidic system while we kept searching microfabrication compatible materials. Through extensive research, we have found that Teflon™-like material (CYTOP®) reveals high hydrophobicity and reduces the surface clogging problem. We coated all microchannels with Teflon and the experimental results showed the rational improvement, which will be shown in Chapter VI.

### **Interconnecting Micro to Macro**

We had a little trouble in connecting microfluidic devices or systems to conventional fluidic instruments such as pressure sensors or reservoirs in test phase. After developing microfluidic components or systems, we needed to test any developed device individually to check whether it is working properly or not. So fluidic interconnection of microdevices to conventional fluidic setups was unavoidable. As disclosed, dead volume could cause air trapping problem and large pressure drops. To overcome this problem, we have developed a new fluidic interconnection technique and we could reduce that issue.

## **Biochemical Assays**

### **Multiplex Problem**

The initial design work of the device anticipated detecting for only one species of analyte. It is a substantially greater problem to detect and identify multiple analytes, requiring either very rapid sequential cycling of the device or a multiplexed approach wherein more than one detection channel is present and simultaneously active. When only one analyte is being detected, identification is not an issue as the detector output is yes/no with orders of probability. When multiple analytes require identification a larger set of permutations is needed in all of the aspects of device design. A multiplexed detection device can easily default to a single channel device, but not vice versa. This type of change is perceived as what is commonly referred to as “mission creep”.

### **Analyte/Detector Mismatch Problem**

We have found difficulties in optimizing our assays to detect different sized analytical targets. A set of capture beads, conjugate, fluidics geometry and assay timing that works well for a molecular analyte such as a protein toxin does not necessarily work well for a particulate analyte such as a bacterium. This is due to the large differences between the analytes in size, complexity, diffusional behavior and hydrodynamic behavior in fluidics. Small molecules such as the fungal toxins, botulin/tetanus toxin and saxitoxin/tetrodotoxin diffuse rapidly and are not affected by shear flow, whereas the bacteria and their spores have essentially no diffusion in the microfluidics environment and detection timeframe, and are greatly affected by shear flow forces; viruses have intermediate behavior. This poses a design and optimization dilemma.

### **The Mixing Problem**

It has been amply shown at the principal investigator meetings and observed by us that very little gross mixing can be achieved within microfluidics. One premise in using magnetic (or non-magnetic) microbeads to capture the analyte of interest is that they are mixed intimately with the suspension that carries the analyte. This is their strength - the mixing causes a very fast three-dimensional search for the analyte within the mixed volume, and so a very high concentration factor when the reacted beads are collected. A critical stage for this detector is where the analyte substances are first captured and concentrated on arrival from the air collector/liquid interface inlet. This does not yet exist and could not be evaluated. Additionally, the beads must be redispersed at least twice - once when they are dispensed from their storage reservoir and once when they have been concentrated after the capture stage. This redispersion of particles is difficult without active turbulent mixing, an action not easily performed in the laminar flow regime of the microchannels.

### **Contrary Magnetic Bead Behavior**

Magnetic microparticles come in a range of sizes and properties. The largest ones, from Dynal and other manufacturers, are 2.8 - 4.5 microns across, have the highest net magnetic attraction force and the most consistent, precise diameters. They suffer from two very serious drawbacks: 1. They settle out of solution quickly, and 2. They stick to things, and each other, when they should not. The settling part is very troublesome for these beads especially in a microfluidics environment. As mentioned above, mixing and redispersion are difficult. The non-specific adhesion, "stiction", of the beads adds to the difficulties. These beads are observed to maximize their contact area with surfaces, promoting their greatest contact with walls, corners and channel features. This is a problem when they are collected into large aggregates by magnetic attraction. They form clumps, which do not redisperse after the magnetic fields decay. Other annoying properties we have observed with the larger beads is that they seem to have remanent magnetism and they have some variable magnetic susceptibility between beads, both properties are denied by the manufacturers. The size of these beads keeps them from having any significant diffusion.

The medium sized beads, from Bangs (USA) and Estapor (France), run in the 0.5-1.0 micron range and are generally more granular and heterogeneous in size. These beads also settle but are not observed to aggregate as much. Direct observation is

difficult because these microparticles are at or below the resolving power of the optical microscope. These beads have a moderate to high magnetic attractive force, but a very low diffusion rate.

The small nanoparticles, 20-60 nanometer diameter, such as those from Miltenyi Biotec (USA) do not settle whatsoever. They are kept in a state of continuous dispersion by Brownian motion. They are coated with a slightly ionized layer which causes a charge repulsion between them, and they do not aggregate. They diffuse very rapidly. Unfortunately, when these particles adhere to a target they form a relatively thin magnetic shell on that particle, and so the net magnetic attraction they can impart to their target is very low.

### **Non-Specific Binding (NSB)**

This term refers to the inappropriate interaction of biochemical species. This phenomenon generally results in interference with the ability to recognize the presence of an analyte. The case we have seen most frequently is the NSB of the enzyme-antibody conjugate to bead and device surfaces, causing an increase of signal in the absence of increased target. We have found some cases of our dendrimer linkers to be a cause of this NSB. The branched-polymer structures have very many tips, each of which is either a positive or negatively charged group, giving them an ion-exchange characteristic. By changing from a positively charged group to a negatively charged one, we were able to significantly decrease this NSB. We have also investigated surface treatments (perfluorinated spin coatings and chemical surface modifications) and solution additives (blockers) to minimize the impact of NSB.

### **The PAPP Stability Problem**

Our substrate that reacts with the AP enzyme to give a detectable chemical is susceptible to breakdown in solution and in storage. We have explored additives and conditions to improve these properties. Antioxidants and free-radical scavengers have increased the PAPP stability but further work is required. Alternative enzyme/substrate systems are under consideration

### **The Electrode Fouling Problem**

This problem so far remains mostly a theoretical concern. The gold surfaces of the detection electrodes can become coated with adsorbed substances such as proteins and be rendered inoperative. By the tactic of controlling exposure of the electrodes only to analyte in the final assay step we have not yet seen serious performance losses from the electrodes. This effect cannot be dismissed however because it is expected to occur only after exposure to 'dirty' solutions and multiple repetitions. Both of these conditions will occur during extended use and field testing but have not yet been checked during the limited operation that our devices have seen.

## **Microcontroller Based Electronic System**

The most significant problem that occurred was that the specifications on the system changed frequently as improving microfluidic components/systems and biochemical assays. The reason was that the electrical needs changed as the research developed in the microfluidic area. This was to have been expected, but we didn't realize the seriousness until we were underway for several months. It constrained our design processes and forced us to broaden our horizons of thinking about how to approach the problem. Ultimately the result of that caused us to come up with a system design that was far better for a research environment in that it was broader in its applicability and usefulness. The down side was that it wasn't as compact as it might have been. Another area of difficulty was the expanded responsibilities to help develop a laboratory system in order for the work on the chemistry to begin before the microfluidic parts were designed. That expanded the work sufficiently to require another student researcher to be added to the electronics team.

## **V. Lessons Learned**

A most valuable experience was the collaboration with other research groups. These groups worked together to explore and understand microfabrication technologies, biochemistry, and electronic control systems. MEMS researchers now consider biochemical issues when they design a system as do biochemists when they develop an assay. Experience obtained from the project can be expanded to design and develop an improved microfluidic based analysis system for various applications in biotechnologies and diagnostics as well as bio-warfare agent detection.

### **Microfluidic Components and Systems**

The most important lesson that we learned is a better understanding on microfluidic systems. Behavior of fluids in micro world is absolutely different from that in macro world. Some physical effects are very significant in microsystems. For instance, surface tension effect which causes malfunction of the system in a specific application.

We learned not only the fabrication and development of microfluidic systems but also valuable techniques to improve our capabilities in MEMS technology such as bonding techniques and microfluidic interconnection techniques. We also expanded our knowledge of biochemistry and related issues for generic biological applications of MEMS technology. We realized that we have to consider a biocompatibility issue of materials or a non-specific binding issue when we design any biochemical analysis system using MEMS technology.

### **Biochemical Assays**

Our two most important experiences are: 1) the difficulty of applying micro-electro-mechanical systems (MEMS) design to a fluidics and biochemistry development cycle, and 2) the non-intuitive behavior of fluids at the micron scales encountered in MEMS devices. Finding the best workable configurations for the MEMS parts, especially with regard to microbeads and analytical biochemistry, requires multiple cycles of testing and refinement. With the use of MEMS components, each cycle is very costly and slowed by the need for multistep clean-room fabrication. Most of our past experience with biochemical assays has required that solutions for incubation and rinsing steps be switched rapidly and easily, and also that mixing be quick and thorough. We have found these premises do not hold in the microscale dimension.

The development of the testing devices was limited mostly by the availability of engineering components and the practical, technical difficulties of microfluidics. The biochemistry of the magnetic microbead-based electroanalytical process was found to both applicable and practical when tested externally and on separate components. The consequences of the biochemical limitations, such as non-specific binding (NSB), electrode fouling and bead stiction, can only be determined within a fully assembled operating system. Operating prototypes were generally not available except for limited intervals at the very end of the program funding period, so these limitations could not be fully assessed. It is a general observation within our own program and of the other

microfluidics efforts that the analytical chemistry has matured much faster than practical microfluidics.

### **Microcontroller Based Electronic System**

In being a part of a large team of researchers in a multidisciplinary project, the most important thing that was learned was that it is absolutely necessary to invest time in the specification phase of the research. That is particularly needed in areas such as electronic systems where the system cannot be changed easily once a direction has been set. While such systems are better understood compared to the other parts of the research, they are more complicated and redesign is very time consuming. Spending more time on setting specifications can pay off later on not only in time savings but also in having a better system.



## VI. Results

All four microfluidic systems have been tested and characterized for both microfluidic performance and biochemical detection capabilities. In biochemical detection tests, mouse immunoglobulin G (IgG) was chosen as a simulant of a biowarfare agent. Both the fully automated integrated microfluidic system and the fully integrated microfluidic systems were successfully developed and characterized by performing full magnetic bead-based immunoassays.

### Automated Integrated Microfluidic Systems for Biochemical Detection

The stand-alone hand-held microfluidic system has been developed and characterized and a sandwich immunoassay has been done in the microfluidic system to detect biohazard species using a generic antigen. The detection of the biomolecule species has been accomplished by performing a magnetic bead-based immunoassay. The system was integrated by using biocompatible silicone tubing for interconnections between the devices. The system consists of four collapsible reservoirs made of very thin bio-compatible polyethylene / Teflon™ with a magnetic bead stirrer, an array of zero dead volume pinch-valves, two new “magnetic curtain” magnetic particle separators, a micro wire electrode/micromachined IDA for detection, a micro flow sensor and a valveless rotary pump as already discussed. The final mini-scale systems are shown in Figure VI-1.

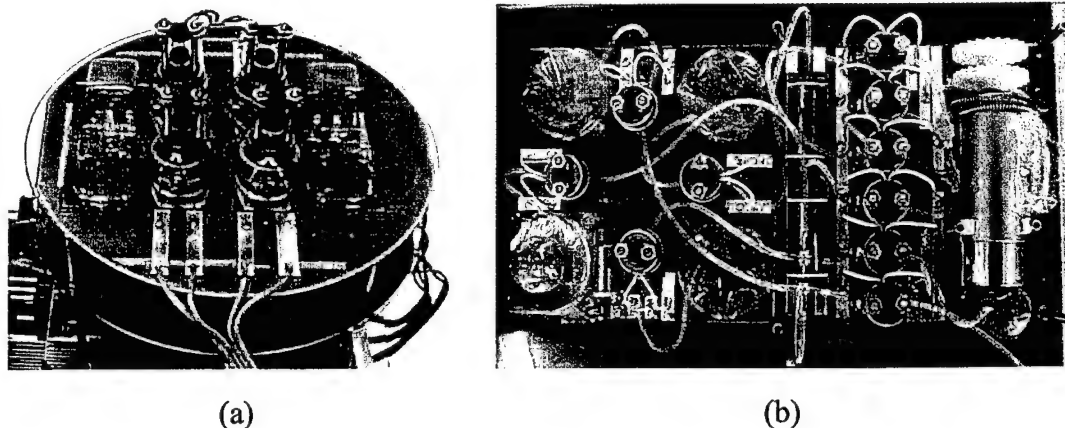


**Figure VI-1: Packaged microfluidic systems**

(a) glass-on-silicon system and (b) silicone system.

The system has proven effective for carrying out sandwich immunoassays on paramagnetic bead surfaces as well as for electrochemically detecting the product formed by the enzyme label. The immunoassay sandwich, formed within the “magnetic curtain” of the first magnetic particle separator, includes the primary antibody attached to the paramagnetic bead surface, and antigen (mouse IgG) captured by the primary antibody, and enzyme-labeled secondary antibody. The enzyme label is responsible for the conversion of PAPP to PAP, within the “magnetic curtain” of the second magnetic

particle separator. Oxidation of PAP at the working electrode surface produces a current, whose amplitude is directly related to the amount of bio-organism present. To establish the relationship of peak current to PAP concentration, PAP with concentrations ranging from  $1.1 \times 10^{-7}$  to  $1.1 \times 10^{-4}$  M in tris buffer were detected in the microfluidic system. The detector used was a thin-layer electrochemical cell consisting of a glassy carbon working electrode held at 290 mV versus a Ag/AgCl reference electrode in a thin-layer flow cell. Figure VI-2 shows the current-time plots produced with detection of PAP. Tris buffer, which both precedes and succeeds the PAP plug, establishes the baseline seen framing the peak current. The log-log plot in Figure VI-3, obtained from the data in Figure VI-2, shows a linear relationship over 4 orders of magnitude, and the peak current is directly related to the amount of PAP in the plug.

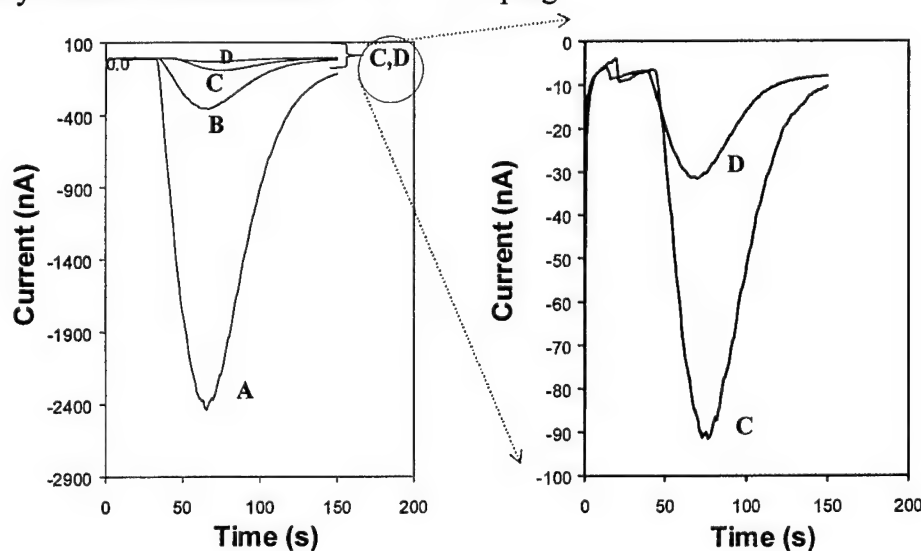


Figure VI-2: Current-time plots for detection of PAP concentrations

(A)  $1.1 \times 10^{-4}$  M, (B)  $1.1 \times 10^{-5}$  M, (C)  $1.1 \times 10^{-6}$  M, and (D)  $1.1 \times 10^{-7}$  M in the mini microfluidic system.

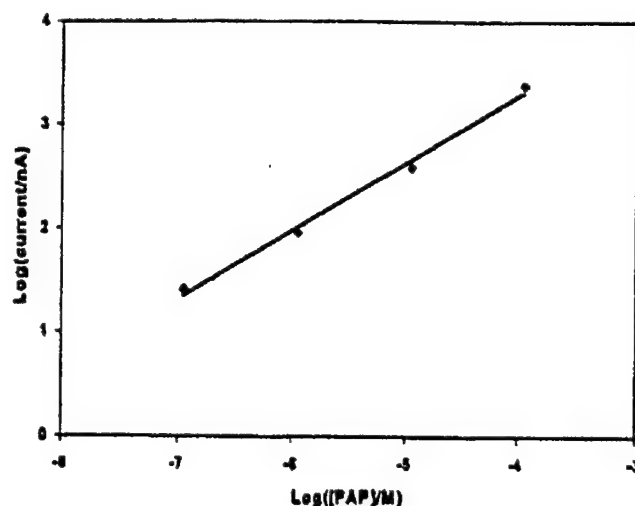


Figure VI-3: Anodic peak current Measured from the baseline current and plotted versus PAP concentration

A sandwich immunoassay calibration curve was obtained using the immunomagnetic beads. PAPP was incubated with the beads for 5 minutes and the PAP produced by enzymatic conversion was detected. The current versus analyte (mouse IgG) concentration plot from the assays are shown in Figure VI-4. The linear relationship spans 3 orders of magnitude. The blank (zero bio-organism concentration) followed the same path as the other samples without the presence of beads.

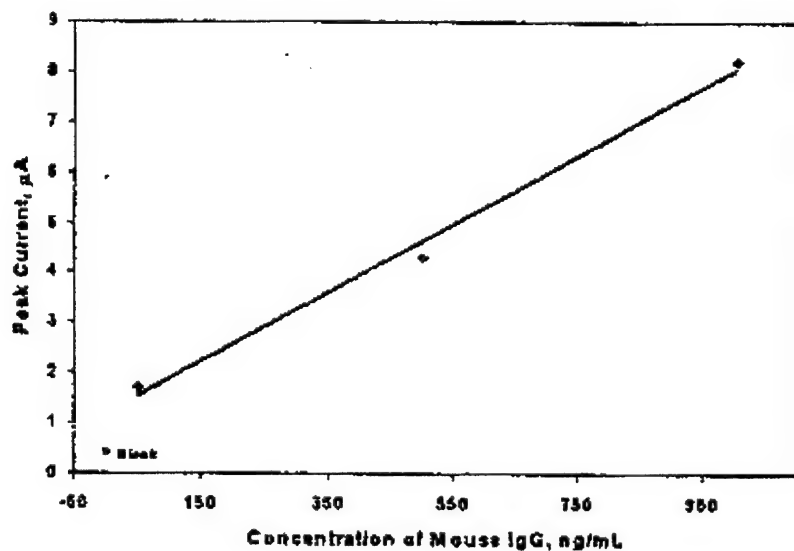


Figure VI-4: Assay calibration curve of amperometric sensing current peaks versus concentration of mouse IgG

## Integrated Microfluidic System for Biochemical Detection

Microfluidic components described in Section 2 of Chapter III were integrated on glass motherboards. Figures VI-5 and VI-6 show four different versions of the microfluidic biochemical detection systems. We have also realized the system on a plastic fluidic motherboard in parallel to glass motherboard systems using commercially available microfluidic valves and pumps to overcome an air-trapping problem in membrane-type microvalves as discussed in Chapter IV.

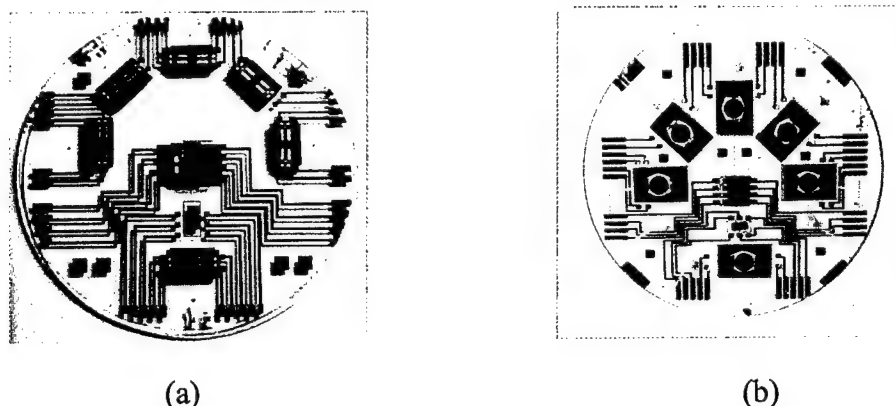


Figure VI-5: Integrated microfluidic systems on 3" glass microfluidic motherboards

Membrane type microvalves were used

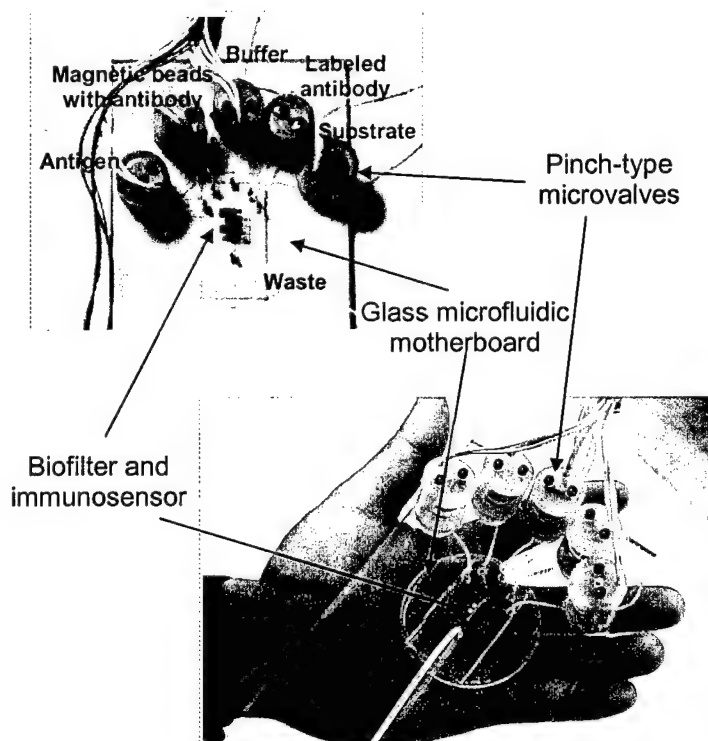
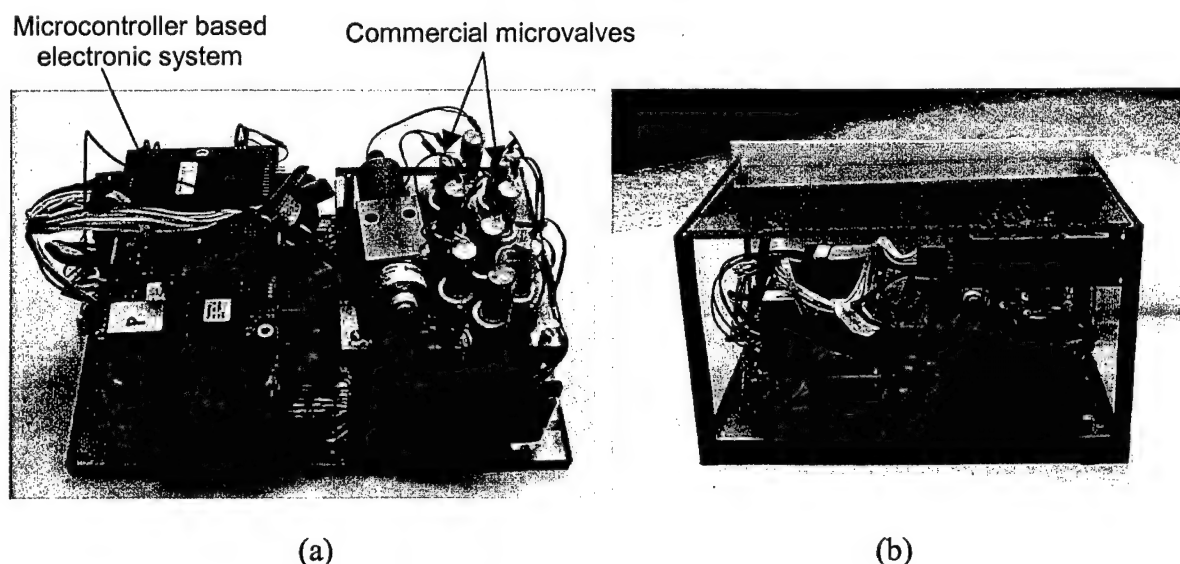


Figure VI-6: Integrated microfluidic system for biochemical detection

The plastic motherboard is created using Polycarbonate (PC). PC is an optically transparent thermoplastic polymer and lends itself well to mechanical machining in addition to being a very cheap motherboard material. A CNC machine was used to create the microfluidic channels on the PC substrate by mechanical engraving. The CNC machine has a tolerance of  $\pm 12.5 \mu\text{m}$  corresponding to approximately 5% tolerance over channel depth and width dimensions. The surface roughness created by mechanical engraving is within the allowable limits for this application. The top PC plate has mechanical fixtures for the microvalves, micropump also created by mechanical machining. The two sides of the PC substrates which come in contact to form the microchannels are then spin-coated with a Teflon® like polymer, CYTOP. CYTOP has poor adhesion when coated directly on PC; therefore we performed a RIE “ashing” step to roughen the surface of the PC. After the RIE operation spin-coated CYTOP films showed good adhesion to the PC substrate. CYTOP coatings were evaluated by the chemistry group and are ideally suited for the present application from biochemical compatibility perspective. Furthermore the intermediate layers of CYTOP are also used as a bonding layer. Since the  $T_g$  (Glass transition temperature for a thermoplastic material) of CYTOP is less than that of PC the bonding occurs without any deformation in the microfluidic channels. The plastic based portable system is shown in Figure VI-7.



**Figure VI-7: Plastic based microfluidic system for biochemical detection**

(a) Assembled all components/systems, and (b) stand alone system (case: 8" x 6" x 6").

For biochemical tests, we chose the system shown in Figures VI-6 and VI-7 since these two systems have no problem in microfluidic performance: i.e. no air trapping inside of the microfluidic channels and fully compatible with developed microcontroller driving/detecting system to construct the targeted stand alone hand-held microfluidic biochemical detection systems. Both systems have different microchannel structures, but the biofilter/immunosensor combination is exactly same.

As discussed in Section 2 of Chapter III, the biofilter and the immunosensor was fabricated separately and integrated together as illustrated in Figure VI-8. The reaction

and sensing chamber volume is 750 nL. The integrated biofilter and immunosensor was surface-mounted using developed fluoropolymer (Teflon™) bonding technique on microfluidic motherboards.

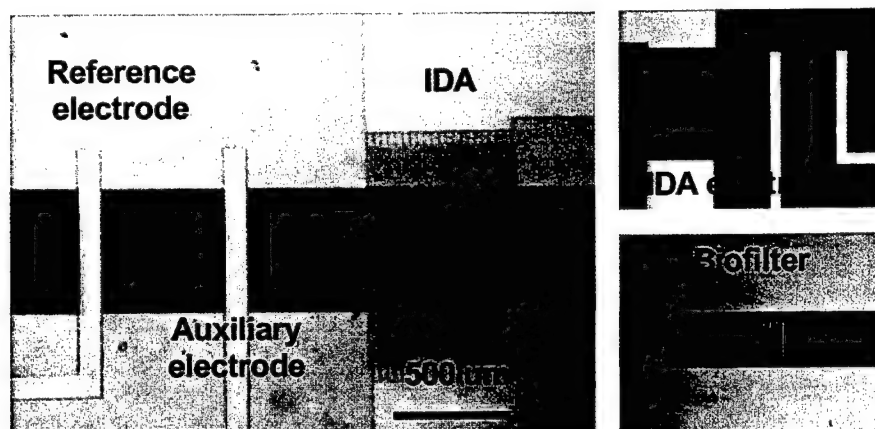


**Figure VI-8: Microphotograph of the integrated biofilter and biosensor**

The volume of the fluidic chamber for biofiltration, reaction, and detection was calculated to 750 nL.

After fluidic sequencing test, full immunoassays were performed in the integrated microfluidic system to prove magnetic bead-based biochemical detection and sampling function followed by calibration of the electrochemical immunosensor. The electrochemical immunosensor was tested and calibrated by flowing PAP solution and the calibration curve of the electro-chemical immunosensor for different PAP concentration is shown in Figure VI-9.

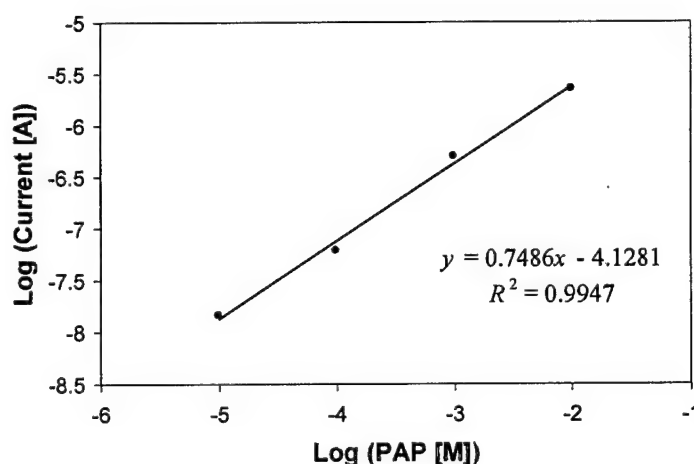


**Figure VI-9: Calibration curve of the electrochemical immunosensor for PAP solution**

Magnetic beads (Dynabeads® M-280, Dynal Biotech Inc., shown in Figure VI-10) coated with biotinylated sheep anti-mouse immunoglobulin G (IgG) were injected into

the reaction chamber and separated on the surface of the biofilter by applying magnetic fields. While holding the magnetic beads, antigen (mouse IgG) was injected into the chamber and incubated. Then secondary antibody with label (rat anti-mouse IgG conjugated alkaline phosphatase) and electrochemical substrate (PAPP) to alkaline phosphatase was sequentially injected and incubated to ensure production of PAP. Electrochemical detection using an amperometric time-based detection method was performed while incubation. After detection, magnetic beads with all reagents were washed away and the system is ready for another immunoassay. The sequence used for the immunoassay is summarized in Table VI-1. This sequence was repeated for every new immunoassay. The flow rate was set to 20  $\mu\text{l}/\text{min}$  in every step.

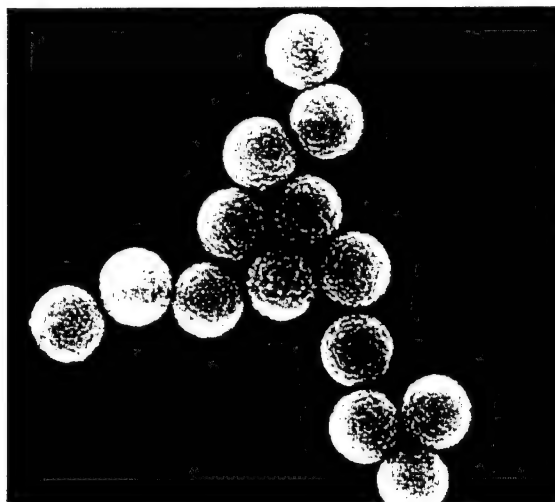


**Figure VI-10: Magnetic beads**

(Dynabeads® M-280. Photograph was provided by Dynal Biotech Inc.). Diameter of the beads is 2.8  $\mu\text{m}$ .

**Table VI-1. Sequence of the magnetic bead-based immunoassay.**

- 1) Injection of primary antibody coated magnetic beads (biotinylated sheep anti-mouse IgG on magnetic beads) for 2 minutes
- 2) Flowing buffer for 30 seconds
- 3) Injection of antigen (mouse IgG) for 30 seconds
- 4) Incubation for 5 minutes
- 5) Flowing buffer for 30 seconds
- 6) Injection of labeled antibody (alkaline phosphatase labeled rat anti-mouse IgG) for 30 seconds
- 7) Incubation for 5 minutes
- 8) Flowing buffer for 30 seconds
- 9) Injection of substrate (PAPP) for 30 seconds
- 10) Incubation for 5 minutes
- 11) Detection for 1 minute
- 12) Flushing everything out
- 13) The system is ready for another assay
- 14) Assay time: *Less than 20 minutes at 20  $\mu\text{l}/\text{min}$  of flow rate*

Full immunoassays were performed following the sequence in Table VI-1 for different antigen concentration: 50, 75, 100, 250, and 500 ng/ml. Concentration of primary antibody coated magnetic beads and conjugated secondary antibody was  $1.02 \times 10^7$  beads/ml and  $0.7 \mu\text{g/ml}$ , respectively. Immunoassay results for different antigen concentration are shown in Figure VI-11.

Immunoreactant consumed during one immunoassay was  $10 \mu\text{l}$  ( $20 \mu\text{l/min} \times 30$  seconds) and total assay time was less than 20 minutes including all incubation and detection steps.

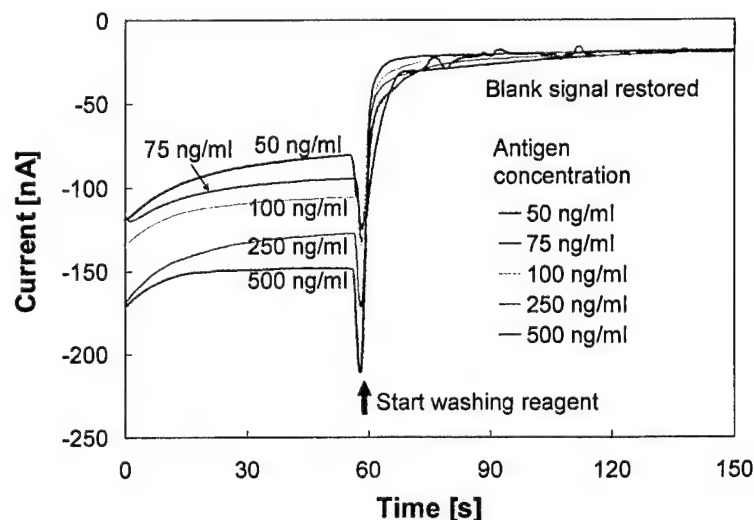


**Figure VI-11: Immunoassay results measured by amperometric time-based detection method**

Immunoreactant consumed during one immunoassay was  $10 \mu\text{l}$  ( $20 \mu\text{l/min} \times 30$  seconds) and total assay time was less than 20 minutes including all incubation and detection steps.

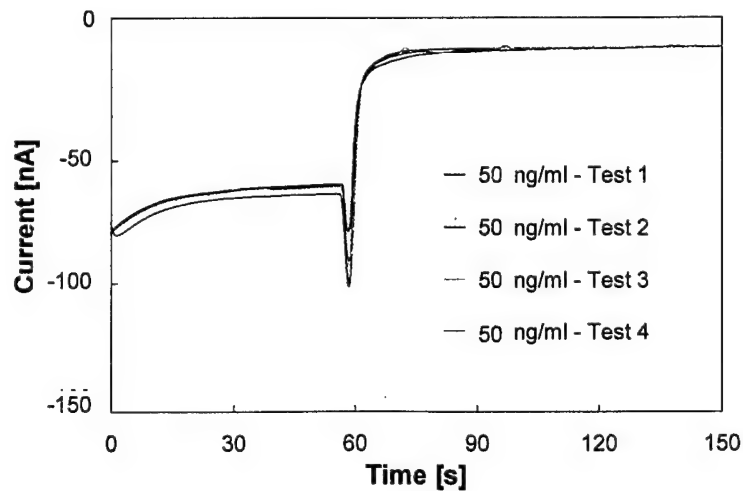


**Figure VI-12: Four repeated immunoassays for 50 ng/ml of antigen concentrations**



Reproducibility of the system was also tested through four times of repeated immunoassay for 50 ng/ml of antigen concentration and the results are shown in Figure VI-12. The repeated immunoassay results in Figure VI-12 shows reliable and stable performances of the integrated microfluidic biochemical detection system developed in this project.

Figure VI-13 shows measurement results from step 6) in Table VI-1 after release of magnetic beads. It is believed that the signal from 0 ng/ml of antigen concentration could be caused by clogging of magnetic beads or non-specific absorption of secondary antibody.

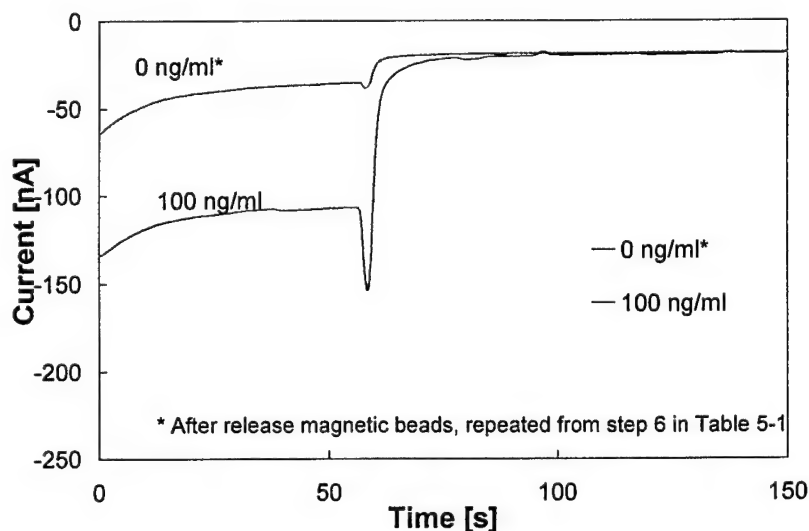


**Figure VI-13: Measurement result after release magnetic beads**

The signal from 0 ng/ml of antigen concentration could be caused by clogging of magnetic beads or non-specific absorption of secondary antibody.

Magnetic bead-based immunoassay, as a typical example of biochemical detection and analysis, has been performed on the integrated micro biochemical analysis system that includes a surface-mounted biofilter and immunosensor on a glass microfluidic motherboard. Protein sampling capability has been demonstrated by capturing target antigens.

Fast (less than 20 minutes) and small volume (10  $\mu$ l) immunoassay has been successfully performed and demonstrated in the integrated biochemical detection system showing promising analysis results. A sample with antigen concentration of 50 ng/ml has been successfully detected by magnetic bead-based immunoassay in the integrated biofilter and electrochemical immunosensor.

## VII. Conclusions

Generic microfluidic systems for biochemical detection have been developed using MEMS technologies and characterized by means of a magnetic bead-based immunoassay in this project. We have eventually realized three microfluidic systems: automated integrated microfluidic system, fully integrated microfluidic system on glass, and plastic based microfluidic system to supplement any possible risks. All of these systems have showed promising results for portable biochemical detection. The realized microfluidic systems have been successfully characterized by performing full immunoassays as a proof concept of the systems using mouse IgG as a simulant of bio-warfare toxic agent. Immunoreactant consumed during one immunoassay was as low as 10  $\mu$ l and total assay time was as low as 20 minutes including all incubation and detection steps. Sample with antigen concentration of 50 ng/ml has also been successfully detected by magnetic bead-based immunoassay with the realized microfluidic systems toward portable biochemical detection.

To realize the microfluidic systems, all microfluidic components such as microvalves/pumps, magnetic biofilters, reservoirs, and microfluidic motherboards have been fabricated and characterized individually in addition to development of related technology like microfluidic interconnection technique and bonding technique. Several prototype microfluidic devices have been designed and developed to verify their capabilities. Consideration on integration issues and biochemical compatibility issues has been extensively explored to achieve the project goal. A microfluidic motherboard approach has been adopted to integrate individually developed microfluidic components such as biofilters, microvalves/pumps, flow sensors, reservoirs, and reaction/sensing cells. A new material like spin-on Teflon™ has been explored and adopted as a device-to-wafer and/or wafer-to-wafer bonding layer. Since both microvalves and biofilters are magnetically operated, magnetic microinductors based on UV-LIGA technique have been also investigated and improved.

The analytical concept is based on an immunoassay with electrochemical detection. Microbead technology is used both in sampling and in detection to trap and manipulate the target molecules. The magnetic beads have been used as both immobilization surfaces and carriers of target bio-molecules. The sensing and detecting format was a sandwich immunoassay using electrochemical detection with the antibody capture surface being on magnetic microbeads. In developing magnetic bead-based assay, various types of molecular linkers have been investigated to improve the speed, capacity and interchangeability of magnetic bead function. Applicability of the bead-based assay to the different types of analyte target has been explored for protein toxin, virus, bacterial spore, and bacterium. Small volume rapid methods of electrochemical assay on microbeads have been also developed for the purpose of magnetic bead-based assay development. The electrochemical immunosensor sensitivity has been enhanced with specially designed microelectrodes configuration and electronic control.

Electronic control systems were developed for the control of microfluidic components (i.e. sequence of microvalves, biofilters), data capture (i.e. electric signal from immunosensor) and analysis aspects of the research. The microfluidic system consisted of up to 10 individual devices, which had to be controlled sequentially and rapidly. The electrochemical detection principle required highly sensitive analyzing

circuitry since the signal level from the electrochemical immunosensor is extremely low. To fulfill these requirements toward a generic microfluidic hand-held system for biochemical detection, a microcontroller board was developed along with a microvalve controller, potentiostat, AD/DA converter, display unit, and an interface board to a PC to download the basic instruction set to the microcontroller. The system was designed so that the main microcontroller board managed the system operation. All parts of the electronic and control system were built using printed circuit boards to minimize the system size and to optimize performance. The stack of boards was quite compact and made a unit suitable for field testing. The complete units were tested and used for biochemical assays in several cases. Some designs were started on an IC version of parts of the system, particularly the analog signal acquisition part.

Combining microfluidic systems, electronic/control circuit systems, and biochemical assays, several stand-alone microfluidic systems for magnetic bead-based biochemical detection have been realized to complete of the project. System volume is approximately 288 in<sup>3</sup> (8 x 6 x 6 inches).

The methodology and system, which has been developed in this project, can be expanded to design and develop an improved microfluidic based analysis system for various applications in biotechnologies and diagnostics as well as bio-warfare detections.

## VIII. APPENDICES

Over 50 papers have been published in journals or presented at numerous international conferences. They are listed in Appendix A.

Total 13 (9 Doctorate and 4 Masters) theses have been published from the project. They are listed in Appendix B.

### Appendix A: List of Publications

1. J.-W. Choi, K. W. Oh, J. H. Thomas, W. R. Heineman, H. B. Halsall, J. H. Nevin, A. J. Helmicki, H. T. Henderson, and C. H. Ahn, "An Integrated Microfluidic Biochemical Detection System with Magnetic Bead-Based Sampling and Analysis Capabilities," Proceedings of the 14<sup>th</sup> IEEE Conference on MEMS (MEMS 2001), Interlaken, Switzerland, January 21-25, 2001, pp. 447-450.
2. S. Dharmatilleke, H. T. Henderson, S. Bhansali, and C. H. Ahn, "Three-Dimensional Silicone Microfluidic Interconnection Scheme Using Sacrificial Wax Filaments," Proceedings of SPIE Micromachining and Microfabrication Conference, Santa Clara, CA, September 18-19, 2000, Vol. 4177, pp. 90-97.
3. J.-W. Choi, C. H. Ahn, S. Bhansali, and H. T. Henderson, "A New Magnetic Bead-Based Filterless Bio-Separator with Planar Electromagnet Surfaces," Sensors and Actuators B, Vol. 68, No. 1-3, August 2000, pp. 34-39.
4. A. Puntambekar and C. H. Ahn, "Self-Aligning Microfluidic Interconnects with Low Dead Volume", Proceedings of mTAS 2000 (4th International Symposium on Micro-Total Analysis Systems), Enschede, The Netherlands, May 13-20, 2000. pp. 323-326.
5. J.-W. Choi, C. A. Wijayawardhana, N. Okulan, K. W. Oh, A. Han, S. Bhansali, V. Govind, K. T. Schlueter, W. R. Heineman, H. B. Halsall, J. H. Nevin, A. J. Helmicki, H. T. Henderson, and C. H. Ahn, "Development and Characterization of a Generic Microfluidic Subsystem Toward Portable Biochemical Detection," Proceedings of  $\mu$ TAS 2000 (4<sup>th</sup> International Symposium on Micro-Total Analysis Systems), Enschede, Netherlands, May 14-18, 2000. pp. 327-330.
6. S. Dharmatilleke and H. T. Henderson, "A Three Dimensional Silicone Device Fabrication and Inter-Connection Scheme for Microfluidic Applications Using Sacrificial Wax Layers," ASME's 2000 International Mechanical Engineering Congress and Exposition, Orlando, FL, November 2000.
7. C. A. Wijayawardhana, W. R. Heineman, H. B. Halsall, C. H. Ahn, T. Henderson, J. H. Nevin, T. Ridgway, C. Lannes, K. Schlueter, J.-W. Choi, S. Bhansali, "A Fully Automated Electrochemical Immunosensor System using Microfabricated Parts," Biosensors 2000 (Sixth World Congress in Biosensors), San Diego, May 24-26, 2000.

8. S. Dharmatilleke, H. T. Henderson, and N. Okulan, "Anodic Bonding of Glass-to-Glass and Silicon-to-Glass or Silicon-to-Silicon through a Very Thick Thermally Grown Silicon Dioxide Layer," International Symposium on Smart Structures & Microsystems (IS<sup>3</sup>M), Hong Kong, China October 19-21, 2000.
9. S. Dharmatilleke, C. A. Wijayawardhana, P. Medis, J. H. Thomas, N. Okulan, H. T. Henderson, W. R. Heineman, and H. B. Halsall, "A Mini/Micro Fluidic System Towards a Generic "Lab-on-a-Chip" to Sample and Detect Airborne Biohazards Via a Biochemical Immunoassay," International Symposium on Smart Structures & Microsystems (IS<sup>3</sup>M), Hong Kong, China, October 19-21, 2000.
10. A. Han, K. W. Oh, S. Bhansali, H. T. Henderson, and C. H. Ahn, "A Low Temperature Biochemically Compatible Bonding Technique using Fluoropolymers for Biochemical Microfluidic Studies", Proc. of the IEEE conf. on Micro Electro Mechanical systems, Miyazaki, Japan, Jan. 23-27, 2000, pp. 414-419.
11. C. A. Wijayawardhana, W. R. Heineman, H. B. Halsall, K. T. Schlueter, T. Ridgway, J.-W. Choi, S. Bhansali, C. Ahn, T. Henderson, C. Lannes, J. Nevin, "An Automated Meso-Scale Immunosensor Towards Lab-on-a-Chip Electrochemical Immunosensing," *Analytical Chemistry*, 2000.
12. S. Kradtap, C. A. Wijayawardhana, K. T. Schlueter, H. B. Halsall, W. R. Heineman, "Bugbead: Artificial Microorganism Model used as a Harmless Simulant for Pathogenic Microorganisms," *Analytical Biochemistry*, submitted 02/22/2000.
13. C. A. Wijayawardhana, G. Wittstock, H. B. Halsall, W. R. Heineman, "Spatially Addressed Deposition and Imaging of Biochemically Active Bead Microstructures by Scanning Electrochemical Microscopy," *Analytical Chemistry* 72: 333-338, 2000.
14. H. B. Halsall, S. Kradtap, C. A. Wijayawardhana, K. Schlueter, W. R. Heineman, "The Bugbead: A Harmless Simulant for Pathogenic Microorganisms," AACC 32<sup>nd</sup> Oak Ridge Conference, Boston, May 5-6, 2000.
15. C. A. Wijayawardhana, S. Purushothama, S. Kradtap, K. Schlueter, H. B. Halsall, T. H. Ridgway, W. R. Heineman, J.-W. Choi, C. Lannes, A. Helmicki, J. Nevin, C. H. Ahn, H. T. Henderson "BioMEMS Immunoassay with Electrochemical Detection," In the Symposium on Immunochemical Methods for the 21<sup>st</sup> Century: Immunochemistry Summit VIII. 219<sup>th</sup> ACS Meeting, San Francisco, CA, March 26-31, 2000.

16. S. Purushothama, S. Kradtap, C. A. Wijayawardhana, K. Schlueter, H. B. Halsall, W. R. Heineman, "Small-Volume Dendrimer Immunomagnetic Bead-Based Assays," Pittcon 2000, New Orleans, March 12-17, 2000.
17. S. Kradtap, C. A. Wijayawardhana, K. Schlueter, H. B. Halsall, W. R. Heineman, "Bug-Bead: An Artificial Microorganism Model as a Harmless Simulant for Pathogenic Microorganisms" Pittcon 2000, New Orleans, March 12-17, 2000.
18. N. Okulan, H. T. Henderson, and C. H. Ahn, "A Pulsed Mode Micromachined Flow Sensor with Temperature Drift Compensation," IEEE Tran. Electron Devices, Vol. 47, February 2000, pp. 340-347.
19. W. R. Heineman, C. A. Wijayawardhana, H.B. Halsall, M. Cousino, S. Purushothama, S. Kradtap, K. Schlueter, T.H. Ridgway, J.-W. Choi, S. Bhansali, C. Lannes, J.H. Nevin, "Immunoassay with Magnetic Beads and Electrochemical Detection," In the Symposium on Electroorganic and Electroanalytical Aspects of Environmental Chemistry. Electrochemical Society Meeting, Honolulu, HI, Oct. 17-22, 1999.
20. W. R. Heineman, H. B. Halsall, T. H. Ridgway, M. Cousino, A. Wijayawardhana, S. Purushothama, S. Kradtap, J.-W. Choi, C. Lannes, J. Nevin, C. Ahn, T. Henderson, "Immunoassay with Novel Electrochemical Detection Methods," 218<sup>th</sup> ACS Meeting, New Orleans, LA, August 22-26, 1999.
21. C. A. Wijayawardhana, H. B. Halsall, W. R. Heineman, "Micro-Volume Rotating Disk Electrode (RDE) Amperometric Detection for a Bead-Based Immunoassay," *Analytica Chimica Acta* 399:3-11, 1999.
22. C. A. Wijayawardhana, S. Purushothama, M. A. Cousino, H. B. Halsall, and W. R. Heineman, "Rotating Disk Electrode Amperometric Detection for a Bead-Based Immunoassay" *Journal of Electroanalytical Chemistry* 468:2-8, 1999.
23. C. H. Ahn, H. T. Henderson, S. Bhansali, J. H. Nevin, A. J. Helmicki, W. R. Heineman, H. B. Halsall, and K. T. Schlueter, "A Portable Biochemical Detection System Using BioMEMS-Based Microfluidic Modules," SERMACS-99, American Chemical Society (ASC), September 19-20, 1999.
24. C. H. Ahn, S. Bhansali, and H. T. Henderson, "Development of A Microfluidic System with Surface Mountable Microfluidic Components for Miniature Biochemical Detection System," Proc. The Pacific/ASME International Intersociety Electronic & Photonic Packaging Conference, INTERpack'99, June 15-19, Hawaii, 1999 (Invited)
25. D. J. Sadler, K. W. Oh, C. H. Ahn, S. Bhansali, and H. T. Henderson, "A New Magnetically Actuated Microvalve for Liquid and Gas Control Application,"

Proc. International Conference on Solid Sensors and Actuators, Transducers'99, Sendai, Japan, 1999.

26. K. W. Oh, C. H. Ahn, and K. P. Roenker "Flip-Chip Packaging Using Micromachined Conductive Polymer Bumps and Alignment Pedestals for MOEMS," IEEE Journal of Selected Topics in Quantum Electronics, 1999.
27. K. W. Oh and C. H. Ahn, "Development of An Innovative Flip-Chip Bonding Technique Using Micromachined Conductive Polymer Bumps," IEEE Trans. on Components, Packaging, and Manufacturing Technology, 1999.
28. N. Okulan, S. Bhansali, A. Han, S. Dharmatilleke, J.-W. Choi, M. Patel, K. W. Oh, H. T. Henderson and C. H. Ahn, "Development of Planar Microfluidic Systems Using Conventional and Low Temperature Assembling Schemes for Components," Proc. The international Mechanical Engineering Conference and Exposition, The Winter Annual Meeting of ASME, Nashville, Tennessee, November 1999.
29. M. Patel, H. T. Henderson, S. Bhansali and C. H. Ahn, "An integrated reservoir for on-chip aqueous storage in microfluidic systems," Proc. The international Mechanical Engineering Conference and Exposition, The Winter Annual Meeting of ASME, Nashville, Tennessee, November 1999.
30. S. Bhansali, A. Han, M. Patel, K. W. Oh, C. H. Ahn and H. T. Henderson, "Resolving chemical/bio-compatibility issues in microfluidic MEMS systems," Proc. SPIE's 1999 Symposium on Micromachining and Microfabrication, Santa Clara, 1999.
31. J.-W. Choi, S. Bhansali, C. H. Ahn, and H. T. Henderson, "A New Magnetic Bead-Based Filterless Bio-Separator with Planar Electromagnet Surfaces," Proc. Eurosensors XIII, The Hague, The Netherlands, 1999. pp. 713-716.
32. D. J. Sadler, K. W. Oh, C. H. Ahn, S. Bhansali, and H. T. Henderson, "A New Magnetically Actuated Microvalve for Liquid and Gas Control Applications," Proc. Transducers '99 (The 10th International Conference on Solid-State Sensors and Actuators), Vol. 2, pp. 1812-1816, Sendai, Japan, June 7-10, 1999.
33. W. R. Heinemann, H. B. Halsall, M. Cousino, C. A. Wijayawardhana, S. Purushathama, S. Kradtap, K. Schlueter, J.-W. Choi, C. H. Ahn, H. T. Henderson, "Electrochemical Immunoassay with Microfluidic Systems," PITCONN'99, Orlando, FL, March 7-12, 1999.
34. Y. Ding, L. Zhou, H. Brian Halsall and W. R. Heineman. "Feasibility Studies of Simultaneous Multianalyte Amperometric Immunoassay Based on Spatial Resolution," *J. Pharm. Biomed. Anal.*, 19, 153-161, 1999.

35. A. Mehta and A. Helmicki, "Design and Control Oriented Modelling of Microfluidic System Components," Proc. of the 1999 American Control Conference, San Diego, CA, June 1999.
36. W. R. Heineman, H. B. Halsall, M. Cousino, A. Wijayawardhana, S. Purushothama, Y. Ding, L. Zhou, J.-W. Choi, C. H. Ahn, T. Hernderson, G. Wittstock, "Electrochemical Immunosensors Based on MEMS Technology", Immunochemistry Summit VII & Third Workshop on Biosensors & Biological Techniques in Environmental Analysis, Las Vegas, NV, December 1-3, 1998.
37. M. A. Cousino, M. Teresa Fernandez-Abedul, M. E. Dotson, H. Brian Halsall, W. R. Heineman, A. R. Pinhas, "A Comparison Between Two Buffer Systems for Enhanced p-Aminophenol Stability," Immunochemistry Summit VII & Third Workshop on Biosensors & Biological Techniques in Environmental Analysis, Las Vegas, NV, December 1-3, 1998.
38. W. R. Heineman, H. B. Halsall, M. A. Cousino, C. A. Wijayawardhana, S. Purushothama, Y. Ding, J.-W. Choi, C. H. Ahn, T. Henderson, "Electrochemical Immunoassay with Microfluidic Systems," Pre-satellite Symposium of the 49th ISE Meeting on the New Trends in Electroanalytical Chemistry, Seoul, S. Korea, Sept. 10-12, 1998.
39. M. A. Cousino, M. T. Fernandez-Abedul, H. B. Halsall, W. R. Heineman, "Comparison Between Two Buffer Systems for Enhanced p-Aminophenol Stability," ACS Central Regional Meeting, Cleveland, OH, May 27-29, 1998.
40. M. E. Dotson, S. Purushothama, M. A. Cousino, H. B. Halsall, W. R. Heineman, A. R. Pinhas, "Small-Volume Immunoassay Development Using Dendrimer-Coated Microspheres as the Solid Support", ACS Central Regional Meeting, Cleveland, OH, May 27-29, 1998.
41. K. D. Kramer, K. W. Oh, C. H. Ahn, J. J. Bao, and K. Wehmeyer "Novel Microchip Format Capillary Electrophoresis (CE) System on Schott Borofloat Glass With Integrated Fiber Optics," Proc. SPIE's 1998 Symposium on Micromachining and Microfabrication, Vol. 3515, 3515-06, Santa Clara, CA, September 21-22, 1998.
42. C. H. Ahn and M. G. Allen, "Micromachined Planar Inductors on Silicon Wafers for MEMS Applications," IEEE Trans. on Industrial Electronics (Special Issue for MEMS), Vol. 45, No. 6, pp. 866-876, 1998.
43. D. J. Sadler, T. M. Liakopoulos, and C. H. Ahn, "A New Micromachined Electromagnet with Electroplated Ni/Fe Permalloy Through-Holes," Proc. 5<sup>th</sup> International Symposium on Magnetic Materials, Processes, and Device (ECS), pp. 377-388, Boston, MA, Nov. 1-6, 1998.



44. C. H. Ahn, T. Henderson, W. Heineman, and B. Halsall, "Development of a Generic Microfluidic System for Electrochemical Immunoassay-Based Remote Bio/Chemical Sensors," Proc. The Micro Total Analysis System (u-TAS) '98 Workshop, pp. 225-230, Banff, Canada, Oct. 13-16, 1998. (Invited)
45. K. W. Oh, C. H. Ahn, "Flip-Chip Packaging With Micromachined Conductive Polymer Bumps," IEEE, 3rd International Conference on Adhesive Joining Technology in Electronics Manufacturing, Binghamton, NY, September 27-30, 1998.
46. D. J. Sadler, T. Liakopolous, J. Cropp, and C. H. Ahn, "Prototype Microvalve Using A New Magnetic Microactuator," Proc. SPIE's 1998 Symposium on Micromachining and Microfabrication, Vol. 3515, 3515-03, Santa Clara, CA, September 21-22, 1998.
47. J.-W. Choi, C. H. Ahn, H. Henderson, "Planar Bio/Magnetic Bead Separator with Microfluidic Channel," Proc. SPIE's 1998 Symposium on Micromachining and Microfabrication, Vol. 3515, 3515-28, Santa Clara, CA, September 21-22, 1998.
48. C. H. Ahn, "Microfluidics and Bio-Microsystems," SEMI Conference on Commercialization of Microsystems 98", San Francisco, CA, September 13-17, 1998. (Invited)
49. K. W. Oh and C. H. Ahn, "Development of An Innovative Flip-Chip Bonding Technique Using Micromachined Conductive Polymer Bumps," Proc. Solid-State Sensor & Actuator Workshop, pp. 170-173, Hilton Head, SC, June 7-11, 1998.
50. N. Okulan, H. T., Henderson, C. H. Ahn, "A New Pulsed-Mode Micromachined Flow Sensor for an Integrated Microfluidic System," Proc. Solid-State Sensor and Actuator Workshop, pp 320-324, June 7-11, 1998.
51. A. Mehta and A. Helmicki, "First Principle Approach to Modelling of Micro-Fluidic System," Proc. SPIE's 1998 Symposium on Micromachining and Microfabrication, Santa Clara, CA, Sept. 1998.
52. W.R. Heineman "Electrochemical Biosensors", 213th ACS National Meeting, San Francisco, CA. April 13-17, 1997 in Symposium on Biosensing and Biosensors: Chemistry, Recognition, and Process Control. Plenary Session II: Topical Reviews.
53. J.-W. Choi, Y. Ding, C. H. Ahn, H. B. Halsall and W. R. Heineman "A Microchip Electrochemical Immunosensor Fabricated Using Micromachining Techniques", in *Proceedings of IEEE EMB Conference* (Inst. of Electrical & Electronics Engineers, Engineering in Medicine & Biology), Chicago, IL, Oct. 29-Nov. 2, 1997, pp. 2264-2266.

54. D. J. Sadler, W. Zhang, C. H. Ahn, H. J. Kim, and S. H. Han, "Micromachined Semi-Encapsulated Spiral Inductors for MEMS Applications," IEEE Trans. on Magnetics, Vol. 33, pp. 3319-3321, 1997.
55. T. Liakopoulos, J.-W. Choi and C. H. Ahn, "A Bio/Magnetic Bead Separator on Glass Chips using Semi-Encapsulated Spiral Electromagnets," Proc. International Conference on Solid Sensors and Actuators, Transducers'97, pp. 485-488, 1997.

## **Appendix B: List of Theses**

1. Trifon M. Liakopoulos (Committee Chair: Chong H. Ahn), "Magnetic MEMS-Based Microstructures and Sensors Using a New Thick Photolithography Technique," Ph.D. Thesis, University of Cincinnati, 2000.
2. Daniel J. Sadler (Committee Chair: Chong H. Ahn), "Development of a New Magnetic Interconnection Technology for Magnetic MEMS Device Applications," Ph.D. Thesis, University of Cincinnati, 2000.
3. Jin-Woo Choi (Committee Chair: Chong H. Ahn), "Magnetic Particle Separators and Integrated Biofilters for Magnetic Bead-Based Biochemical Detection System," Ph.D. Thesis, University of Cincinnati, 2000.
4. Kwang Wook Oh (Committee Chair: Chong H. Ahn), "Development of Magnetically Actuated Microvalves and Micropumps for Surface Mountable Microfluidic Systems," Ph.D. Thesis, University of Cincinnati, 2000.
5. Nihat Okulan (Committee Chair: H. Thurman Henderson), "Fabrication and Characterization of a Pulsed MEMS-Based Micro Flow Sensor for Microfluidic Application," Ph.D. Thesis, University of Cincinnati, 2000.
6. Saman Dharmatilleke (Committee Chair: H. Thurman Henderson), "MEMS Prototypical System Integration and Packaging for a Generic Microfluidic System," Ph.D. Thesis, University of Cincinnati, 2000.
7. Supaporn Kradtap (Committee Chair: William R. Heineman and H. Brian Halsall), "I. Development of Bead-Based Sandwich Immunoassays with Electrochemical Detection for Harmless Simulants, II. Procedures to Improve Sandwich Immunoassay Performance," Ph.D. Thesis, University of Cincinnati, 2000.
8. Shobha Purushothama (Committee Chair: William R. Heineman and H. Brian Halsall), "Development of Immunomagnetic Bead Assay with Electrochemical Detection for Use in a Miniaturized Sensor," Ph.D. Thesis, University of Cincinnati, 2001.

9. C. Ajith Wijayawardhana (Committee Chair: William R. Heineman and H. Brian Halsall), "Rapid Microimmunoassay with Electrochemical Detection," Ph.D. Thesis, University of Cincinnati, 2001.
10. Sreenevasan Ranganathan (Committee Chair: H. Thurman Henderson), "Applications of Coherent Porous Silicon (CPS) Technology in Micro-Fluidic Systems," M.S. Thesis, University of Cincinnati, 2000.
11. Vinu Govind (Committee Chair: Joseph H. Nevin), "Interface Circuits and Systems for Microfluidic Components," M.S. Thesis, University of Cincinnati, 2000.
12. Preethy Nagendran (Committee Chair: Joseph H. Nevin), "System Control and Integration for Stand Alone Micro Fluidic Systems," M.S. Thesis, University of Cincinnati, 2000.
13. Muralimanohar Vepadharmalingam (Committee Chair: Joseph H. Nevin), "Design of a Dual Working Electrode Potentiostat for Remote Biosensors," M.S. Thesis, University of Cincinnati, 2000.

***MISSION  
OF  
AFRL/INFORMATION DIRECTORATE (IF)***

*The advancement and application of Information Systems Science  
and Technology to meet Air Force unique requirements for  
Information Dominance and its transition to aerospace systems to  
meet Air Force needs.*